STP 591

RESISTANCE TO PLANE-STRESS FRACTURE (R-CURVE BEHAVIOR) OF A572 STRUCTURAL STEEL

S. R. NOVAK

AMERICAN SOCIETY FOR TESTING AND MATERIALS

RESISTANCE TO PLANE-STRESS FRACTURE (R-CURVE BEHAVIOR) OF A572 STRUCTURAL STEEL

Presented at
Eighth National Symposium
on Fracture Mechanics,
Brown University,
Providence, R. I., 26-28 Aug. 1974

ASTM SPECIAL TECHNICAL PUBLICATION 591

S. R. Novak
U. S. Steel Corporation
Research Laboratory

List price $5.25
04-591000-30

AMERICAN SOCIETY FOR TESTING AND MATERIALS
1916 Race Street, Philadelphia, Pa. 19103

Library of Congress Catalog Card Number: 75-18414

NOTE
The Society is not responsible, as a body,
for the statements and opinions
advanced in this publication.

Printed in
New Carlisle, Ohio
February 1976

Foreword

This publication, Resistance to Plane-Stress Fracture (R-Curve Behavior) of A572 Structural Steel, is one of the papers presented at the Eighth National Symposium on Fracture Mechanics which was held at Brown University, Providence, R. I., 26-28 Aug. 1974. A summary only appears in the proceedings of this symposium (Mechanics of Crack Growth, ASTM STP 590). The symposium was sponsored by Committee E-24 on Fracture Testing of Metals of the American Society for Testing and Materials. J. R. Rice and P. C. Paris, Brown University, presided as symposium co-chairmen.

Related ASTM Publications

Mechanics of Crack Growth, STP 590 (1976), $45.25, 04-590000-30

Fracture Analysis, STP 560 (1974), $22.75, 04-560000-30

Fracture Toughness and Slow-Stable Cracking, STP 559 (1974), $25.25, 04-559000-30

Fatigue and Fracture Toughness—Cryogenic Behavior, STP 556 (1974), $20.25, 04-556000-30

A Note of Appreciation to Reviewers

This publication is made possible by the authors and, also, the unheralded efforts of the reviewers. This body of technical experts whose dedication, sacrifice of time and effort, and collective wisdom in reviewing the papers must be acknowledged. The quality level of ASTM publications is a direct function of their respected opinions. On behalf of ASTM we acknowledge with appreciation their contribution.

ASTM Committee on Publications

Editorial Staff

Table of Contents

STP591-EB/Feb. 1976

RESISTANCE TO PLANE-STRESS FRACTURE (R-CURVE BEHAVIOR) OF A572 STRUCTURAL STEEL

By S. R. Novak

Abstract

The R-curve behavior of A572 Grade 50 steel was established over the temperature range -40 to +72 F by using state-of-the-art procedures. Both linear-elastic-fracture-mechanics (LEFM) and crack-opening-stretch (COS) analytical techniques were used in assessing experimental results obtained under load-control and displacement-control testing conditions. This study represents a pioneer effort in that it is the first known attempt to evaluate the R-curve behavior of a low-strength structural steel in some depth.

Results showed a steep K_c transition behavior for 1.5-inch-thick (38 mm) plate, with minimum K_c values of 57, 155, and 318 ksi $\sqrt{\text{inch}}$ (63, 171, and 350 $MNm^{-3/2}$) obtained at -40, +40 and +72 F (-40, +4.5, and +22 C), respectively. A similar behavior was observed for 0.5-inch-thick (12.7 mm) plate, with minimum K_c values of 150, 273, and >380 ksi $\sqrt{\text{inch}}$ (165, 300, and >418 $MNm^{-3/2}$) obtained at the corresponding test temperatures. The results are discussed in relation to the influence of material and testing method, as well as in relation to earlier K_{Ic} results obtained at cryogenic temperatures.

The minimum K_c values measured demonstrate extensive crack tolerance for A572 Grade 50 steel under all combinations of the test conditions studied. With one exception, these minimum behaviors can be translated into total critical flaw lengths that are at least 7 times the plate thickness ($2a_{cr} \geq 7B$) for cracks embedded in large planar structures and subjected to tensile-stress levels equal to 3/4 the yield strength. The applicability of a_{cr} calculations obtained from R-curve measurements generally, and on the A572 Grade 50 steel specifically, is discussed in relation to typical structural members such as H-beams.

Introduction

The ability of linear-elastic fracture mechanics (LEFM)* to successfully predict the onset of catastrophic fracture in metals is well known. The success of this approach derives from the quantitative and accurate manner in which the interchangeability of stress (σ) and flaw size (a) at fracture is predicted. The critical-stress-intensity parameters resulting from the LEFM approach are K_{Ic} to characterize fracture under plane-strain conditions ($\varepsilon_{zz} = 0$) with attendant small-scale crack-tip plasticity, and K_c to characterize fracture under plane-stress conditions ($\sigma_{zz} = 0$) with attendant large-scale crack-tip plasticity. Thus, the behavior represented by K_c is the opposite extreme of that represented by K_{Ic}—that is, negligible rather than complete through-thickness elastic constraint (stress) at fracture. The K_c value is generally 2 to 5 times larger than K_{Ic} and varies not only with temperature (T) and strain rate ($\dot{\varepsilon}$), as does K_{Ic}, but with plate thickness (B) as well. Furthermore, for fixed conditions of temperature, strain rate, and plate thickness (T, $\dot{\varepsilon}$, and B), the K_c value will also vary with initial crack length, a_o.

The operating temperatures, rate of loadings, and thickness of most steel plates used in actual structures are generally such that plane-stress rather than plane-strain conditions actually exist in service. Consequently, the present work was conducted to study the

---

* The nomenclature for the various terms used in this paper is given in the Glossary.

fracture behavior of a typical structural steel under generalized plane-stress conditions.

The fundamental property for determining the variation in K_c with crack length, a_o, is the so-called "R-curve" (resistance curve). The R-curve is a plot of K_R vs Δa (alternatively, G_R vs Δa) and K_R represents the driving force required to produce stable crack extension (Δa) prior to complete catastrophic fracture at K_c. The K_c value that results for a given crack length, a_o, is the value associated with the point of tangency between the line representing the applied load and the R-curve itself, Figure 1.

A volume describing the state-of-the-art of R-curve testing has recently been published.[1)*] Of particular interest as part of this book is a paper by Heyer,[2)] which presents a literature survey of R-curve testing, including some noteworthy historical aspects.

In elementary terms, R-curves can be determined by using either of two experimental methods—"load control" or "displacement control." The load-control technique can be used to obtain only that portion of the R-curve up to the K_c value (where complete unstable fracture occurs), whereas the displacement-control technique can be used to obtain the entire R-curve and therefore offers a fundamental advantage. The equivalence of the two techniques for determining K_c has been demonstrated by the work of Heyer and McCabe,[3,4)] the originators of the displacement-control technique. However, this demonstration of equivalence for the two test tech-

---

* See References.

niques has generally been restricted to high-strength steels and aluminum alloys, where the principles of LEFM are directly applicable as a result of limited crack-tip plasticity. The procedure for evaluating R-curves by using LEFM concepts directly is straightforward, and a recommended practice is currently being prepared by the ASTM.[5]

The evaluation of R-curves for relatively low-strength, high-toughness alloys is more complex. Because such materials exhibit large-scale crack-tip plasticity (r_p) at fracture, relative to the test-specimen in-plane dimensions (W and a), LEFM principles cannot be applied directly. As a consequence, a nonlinear, elastic-plastic approach is required. In this elastic-plastic approach, the crack-opening displacement (δ) at the physical crack tip is measured and used in calculating the equivalent elastic K value.* This nonlinear approach is based on theoretical considerations advanced earlier by Wells[6] and reviewed more recently by Wells[7] and Irwin.[8] This elastic-plastic crack model is designated the crack-opening-stretch (COS) method, where δ and COS are equivalent terms. The application of the COS analysis method to R-curve testing has been developed to an advanced degree by Heyer and McCabe.[9] Furthermore, this method can be used with either the load-control or displacement-control test procedures. The method by which the δ or COS value is measured at the physical crack tip is an offshoot of the "double-compliance" procedure, Figure 2.

* The equivalent elastic K value is the analog K value that would be measured under elastic conditions for which LEFM principles can be used directly when specimens of the same thickness, B, but much larger planar dimensions, W and a, are tested.

The present paper describes a study of the R-curve (plane-stress fracture toughness) behavior of ASTM A572 Grade 50 steel over the temperature range from -40 F to +72 F. The primary reason for this R-curve study was the earlier inability to measure valid K_{Ic} behavior over this same -40 to +72 F temperature range for plate thicknesses typically used in service.[10)] The study was conducted to evaluate the effects of test technique (load control versus displacement control), temperature, and thickness on R-curve behavior. The current study is unique in that it was conducted on a constructional steel that is widely used in many large structures such as bridges.

Basic Elements of R-Curves

An R-curve is, by definition, a plot of K_R vs Δa which characterizes the fundamental resistance to fracture of a given material and plate thickness, B, under plane-stress conditions. The K_R value is always calculated by using the effective crack length, a_{eff}, and is plotted against the actual crack extension, Δa_{act}, that takes place physically in the material during the test. This is true no matter which type of loading technique (load control or displacement control) is used to generate the basic data.

Under plane-strain conditions, the fracture toughness of a material depends on only two variables [$K_{Ic} = f(T \text{ and } \dot{\varepsilon})$], whereas under plane-stress conditions, the fracture toughness depends on four variables [$K_c = f(T, \dot{\varepsilon}, B, \text{ and } a_o)$]. For fixed test and material conditions (T, $\dot{\varepsilon}$, and B), a K_c value merely represents a singular point on an R-curve. On the other hand, an R-curve describes the complete variation of K_c with changes in (initial) absolute crack length, a_o. As such, a single R-curve is a highly efficient method of fracture characterization since it is equivalent to a large number (15 or 20) of direct K_c tests conducted with various (initial) crack lengths, a_o. Thus, the R-curve is the most general characterization of plane-stress-fracture behavior and depends on only three variables [R-curve = f(T, $\dot{\varepsilon}$, and B)].

Materials, Experimental Work, and Analysis

Materials

The steel used in this study was ASTM A572 Grade 50 steel with two strength gradients, 50-ksi (345 MN/m^2) and 62-ksi (425 MN/m^2) yield strength (σ_{ys}), as obtained from two different steel heats. The chemical composition and mechanical properties of each steel are presented in Tables I and II, respectively.

Each of these two A572 Grade 50 steels was obtained as typical, commercially produced 1.5-inch-thick (38 mm) plate. The majority of the present R-curve tests were conducted on the lower-strength (50 ksi) steel, with only a few tests being conducted on the higher-strength (62 ksi) steel. However, the fracture behavior of both steels has been characterized extensively in the laboratory earlier by using a wide range of specimen types (including those for K_{Ic}) and test conditions.[10)] In addition, the laboratory fracture behavior of the lower strength (50 ksi) steel has also been correlated with the fracture behavior of full-scale H-beams (members fabricated with the same 1.5-inch-thick plate) tested under simulated field conditions.[11)]

Test Specimens and Conditions

All specimens used in the investigation were of the compact-tension (CT) type, with $(\frac{H}{W}) = 0.600$; the same basic specimen type is very often used to determine K_{Ic}.[12)] All CT specimens were of the L-T crack orientation* and were tested under "static" loading conditions ($\dot{\varepsilon} \cong 10^{-5}$ to 10^{-4} sec^{-1}) in the temperature range -40 to +72 F (-40 to +22 C).

Two different types of CT specimens were used in the study as shown in Figure 3. The specimens tested under load-control conditions were those with in-plane dimensions corresponding to the 2T and 4T specimen designations, Figure 3A. The "T" denotes that the specimen is tested in tension (with two loading pins), and the preceding number denotes the size of the specimen dimensions relative to those for a 1T specimen (W = 2.00 inches or 51 mm, H = 0.600 W, and a = 0.30 W). The specimens tested under displacement-control conditions were those with in-plane dimensions corresponding to the 4C and 7C specimen designations, Figure 3B. The "C" denotes that the specimen is loaded by a wedge at the crack line, and the preceding number is again the magnification number for the specimen dimensions relative to a 1C specimen (W = 2.00 inches, H = 0.600 W, and a = 0.30 W).

---

* The L-T crack orientation corresponds to that of a full-thickness crack stressed parallel to the rolling direction, L, and propagating across the plate width, T, that is, perpendicular to L.

A total of 24 CT specimens were prepared and tested in the investigation. Of this total, 14 specimens (2T and 4T designation) were tested under load-control conditions and 10 specimens (4C and 7C) were tested under displacement-control conditions, Table III. This total included 14 full-thickness (B = 1.5 inches) specimens for the 50-ksi yield-strength steel to determine the effects of both specimen in-plane dimensions (W and a) and loading technique. Eight additional subthickness (B = 0.5 inch or 12.7 mm) specimens were tested for this same 50 ksi steel to determine the effect of thickness on R-curve behavior. For the 62-ksi yield-strength steel, only two specimens were tested--both 7C in size and full-plate thickness (B = 1.5 inches). All specimens were tested at nominal test temperatures of -40, +40, or +72 F (-40, +4.5 or +22 C).

All 24 CT specimens were prepared prior to test in the same manner. That is, all specimens were prepared with an electrical-discharge-machined (EDM) notch tip ($\rho \leq 0.007$ inch or 0.178 mm), to facilitate fatigue precracking, and all specimens were fatigue-cracked under constant-load (P = constant) test conditions in a 300-kip (1.33 MN) MTS machine. The size of the fatigue-precracking ligament was approximately the same for all specimens ($\Delta a \cong 1/2$ inch), and the preparation such that the final fatigue crack for each specimen was maintained in the range $(\frac{a}{W}) = 0.36$ to 0.45. Furthermore, all 24 specimens were prepared under zero-to-tension sinusoidal loading conditions ($R \cong 0$) at a frequency of 1.0 cycle per second (cps) and in such a manner that the final ΔK_f value (based on final fatigue crack length, a) was nominally maintained in the range $\Delta K_f = 20$ to 35 ksi $\sqrt{\text{inch}}$ (22 to 38.5 $MNm^{-3/2}$).

After precracking, the specimens were tested under either load-control or displacement-control conditions at the assigned test temperatures. The 14 specimens tested under load-control conditions were evaluated at the U. S. Steel Research Laboratory by using a 440-kip (1.96 MN) Baldwin tension-testing machine. The remaining 10 specimens tested under displacement-control conditions were evaluated at the Armco Steel Corporation Research Laboratory located in Middletown, Ohio, by using a specially constructed test machine capable of crack-line loading large specimens with a wedging device.[3,4,9)]

A combined "double compliance" and "COS" procedure was used with both testing methods, Figure 2. In particular, two clip gages were used to measure the displacements V_1 and V_2 at the positions shown in Figure 3B. These values were recorded continuously by using an X-Y recorder and associated signal conditioners. The loading for most specimens was essentially monotonic, with the specimen being partially unloaded at intermittent levels in order to locate the actual crack length (a_{act}). This was done by using the elastic unloading slope in the V_1 vs V_2 test record, denoted as $\left(\frac{V_1}{V_2}\right)_s$. For low values of applied stress intensity, K_I, where the specimen loading is predominantly elastic, the corresponding value of the effective crack length (a_{eff}) was obtained by using the absolute values of V_1 and V_2 measured just prior to the unloading step, denoted as $\left(\frac{V_{1\ abs}}{V_{2\ abs}}\right)$. The details for making such measurements (a_{act} and a_{eff}) by using the "double-compliance calibration procedure" are described elsewhere.[4,5,9)]

Most specimens were tested in the standard manner described above. The only deviation from this procedure occurred in the manner of the load (P) application for the seven 4T specimens (both 0.5 and 1.5-inch thickness) tested under load-control conditions. In these tests, the specimen was also removed from the test machine periodically for additional supplementary measurements at P = 0 conditions.

Direct measurements of the load, P, were made continuously for all load-control tests. Because of frictional considerations, direct measurements of the load could not be made for the deflection-control tests. Accordingly, calculation procedures had to be adopted for these latter tests.

Analytical Techniques

The point of demarcation between LEFM behavior and the nonlinear COS behavior is the occurrence of specimen back-surface yielding ($\varepsilon_{BS} = \varepsilon_{ys} + 0.002$). The analytical procedures for characterizing K_R in each regime of behavior are given below.

LEFM Technique. For $\varepsilon_{BS} < \varepsilon_{ys} + 0.002$, the K_R is calculated by using the normal equation* for a CT specimen,[12)] given as

$$K_R = \frac{P \cdot f(\frac{a}{W})}{B \cdot W^{1/2}} \tag{1}$$

where $f(\frac{a}{W})$ is a specific function of the relative crack length. The value of "a" used in this equation is a_{eff}, described in a preceding section.

COS Technique. For $\varepsilon_{BS} > \varepsilon_{ys} + 0.002$, the K_R value is calculated at any point by first establishing the hinge point, h, using the relationship

$$h = \left[\frac{0.1576W + 0.303W\left(\frac{V_{1\ abs}}{V_{2\ abs}}\right)}{\left(\frac{V_{1\ abs}}{V_{2\ abs}}\right) - 1}\right] \tag{2}$$

The value of h is then used to calculate the COS (or δ) value at the tip of the actual crack length (a_{act}), Figure 2, by using the relation

$$\delta = V_{2\ abs}\left(\frac{h - a}{h - 0.303W}\right) \tag{3}$$

and δ is used, in turn, to calculate the equivalent elastic-stress-intensity value, K_R, by the relation[6,7,8)]

---

* The cited equation applies for any CT specimen, defined by the ratio of the in-plane dimensions $(\frac{H}{W}) = 0.600$, regardless of specimen thickness, B. Accordingly, this relationship is valid for relatively thick (plane-strain) or relatively thin (plane-stress) CT specimen studies.

$$K_R = \left(E \cdot \sigma_{ys} \cdot \delta\right)^{1/2} \tag{4}$$

where E and σ_{ys} are the modulus of elasticity and the yield strength of the material being tested, respectively.

Results and Discussion

1. R-Curve Results

1A. Summary of Basic Behavior. The results obtained from all 24 R-curve tests are presented in summary form in Tables IV and V. Table IV gives a complete characterization of each test strictly in terms of LEFM parameters, regardless of whether LEFM or COS analysis was necessary to quantitatively characterize the point of fracture instability, K_c. Table V gives a summary of all R-curve and K_c results in terms of the appropriate LEFM or COS method of analysis. The specific method of analysis (LEFM or COS) used for calculating K_c is listed for each specimen in Table V. The basis for the choice of analysis at K_c is given in Table IV. The results from all 24 R-curve tests will be discussed in separate sections below.

1B. Effects of Temperature for B = 1.5-Inch Specimens. The individual R-curves obtained for all B = 1.5-inch (38 mm) specimens of the 50 ksi steel tested at nominal temperatures of -40, +40, and +72 F are presented in Figures 4, 5, and 6, respectively. The two R-curves obtained for the 62-ksi steel are presented in Figure 7. The crack extension, Δa, shown in all such R-curve plots of the present study corresponds to actual crack extension ($\Delta a = \Delta a_{act}$) as determined with double-compliance calibration procedures.

The results in Figures 4 through 6 show, collectively, that a rapid increase in plane-stress crack tolerance occurs with increasing temperature. Evidence for this can be seen in both the increasing amounts of stable crack extension preceeding fracture, Δa_c, and the increasing K_c values that occur with increasing temperature. The specific variation in K_c values with temperature for all the B = 1.5-inch specimens tested is presented in a summary plot, Figure 8. This figure shows that the K_c transition is quite steep at temperatures above 0 F (-18 C).

Figure 8 also shows that, within the limitations of evaluation based on only two specimens, the K_c behavior of the 62-ksi steel is the same as that for the 50-ksi steel. This result is surprising to some extent, since the static K_{Ic} transition temperatures for these same two steels are somewhat different.[10)] Comparisons of K_c and K_{Ic} for each of the two steels will be treated in detail in a separate section (2F) below. It is sufficient for the present to note that a "pop-in" behavior was observed for the 62-ksi steel at +72 F. This classical R-curve behavior for the 62-ksi steel was unique in the present study and occurred at a K_R value of approximately 120 ksi $\sqrt{\text{inch}}$ (132 $MNm^{-3/2}$) compared with complete fracture at a K_c value of 365 ksi $\sqrt{\text{inch}}$ (400 $MNm^{-3/2}$), a level 3 times higher.

Several additional features should be noted in the summary plot of K_c behavior, Figure 8. The first is the existence of a relatively wide "scatter band" in the K_c results obtained. This is an important consideration that will be discussed separately in a subsequent section (2A). The second feature is the extremes in behavior exhibited by the 2T and 7C specimens of the 50-ksi steel tested at +72 F. That is, the 2T specimen fractured at an apparent K_c value in excess of 87 ksi $\sqrt{\text{inch}}$ (96 $MNm^{-3/2}$), whereas the 7C specimen did not fail at a K_R value of 477 ksi $\sqrt{\text{inch}}$ (525 $MNm^{-3/2}$), the limit of the test-machine capacity, Table V.

The result for the 7C specimen tested at +72 F is indicative of true material behavior, but the result for the 2T specimen tested at +72 F is not. Rather, the 2T specimen result is a spurious reflection of the method of testing and analysis. Because of the critical nature of this point these results must be described in some detail. First of all, the 2T specimen result at +72 F can be seen to be clearly inconsistent with the results obtained from the same 2T size specimens tested at lower temperatures (-40 and +40 F), Figure 8. The untypical nature of the result at +72 F resulted primarily from limitations in the ability to accurately analyze K_I at fracture. That is, both of the 2T specimens tested at lower temperatures exhibited relatively large amounts of plasticity and required analysis by COS, Tables IV and V. On the basis of these lower temperature results, extensive plasticity and deviation from linearity in the P vs V_1

test record were expected at +72 F. However, the 2T specimen at +72 F fractured prematurely at a 15.5 percent secant intercept value in the P vs V_1 test record prior to the first scheduled partial unloading step--thereby precluding meaningful COS analysis at fracture instability. Despite the nearly linear nature of the P vs V_1 test record, the K_I value at fracture calculated on the basis of LEFM (the only alternative analysis method) was also not meaningful because it was substantially in excess of the various universally accepted limits for LEFM calculations. In particular, as shown in Table IV, the value at fracture for the 2T specimen at +72 F calculated on the basis of LEFM, $K_{I,max} = 91.3$ ksi$\sqrt{\text{inch}}$, was well above both the limit for plane-strain calculations, $K_{I,Lub} = 38.9$ ksi$\sqrt{\text{inch}}$, and each of the conservative limits for plane-stress calculations $K_{MC} = 53.3$ ksi$\sqrt{\text{inch}}$ and $K_{BSY} = 69.7$ ksi$\sqrt{\text{inch}}$. When conditions are such that these LEFM limits are substantially exceeded due to material behavior—as in the present case—calculations based on LEFM have no physical significance because they grossly underestimate the true material behavior in terms of K_I.[10,13,14] This is, of course, the exact reason why COS analysis of such elastic-plastic fracture behavior is necessary for tough materials. However, the value at fracture for the 2T specimen at +72 F calculated on the basis of COS using specific approximations, $K_R \geqq 87$ ksi$\sqrt{\text{inch}}$, Table V, represents a lower bound that is even less than that based on LEFM ($K_{I,max} = 91.3$ ksi$\sqrt{\text{inch}}$) and thus even less meaningful. The reasons for this behavior are currently unknown.

Thus, the conclusion is that the K_c value for the 2T specimen tested at +72 F is invalid, and accordingly, that the results (calculated on the basis of either LEFM or COS) are suppressed in a manner similar to that in which invalid K_{Ic} (K_Q) results become suppressed when specimen dimensions are inadequate.[10,13,14] This artificially lower K_c result from COS appears to be a specific consequence of the violation of both the minimum specimen size and the minimum specimen proportions required for valid COS results (presently undefined).

The greater resistance to fracture exhibited by the A572 steels with increasing temperature in Figure 8 is also confirmed by examining the fracture surfaces of the 2T and 4T CT specimens (tested under load-control conditions), Figures 9 and 10, respectively. The size of the 2T and 4T specimens tested at +72 F in relation to the size of the corresponding 7C specimen tested at the same temperature is illustrated in Figure 11. This figure also illustrates the extensive crack tolerance exhibited by the 7C specimen at the point where the test was terminated without specimen failure ($\Delta a \cong 0.60$ inch or 15 mm on the specimen surface at $K_R = 477$ ksi $\sqrt{\text{inch}}$ or 525 $\text{MNm}^{-3/2}$). The K_c value for this 7C specimen of the 50-ksi steel tested at +72 F is thus in excess of 477 ksi $\sqrt{\text{inch}}$. This compares with a K_c value of 365 ksi $\sqrt{\text{inch}}$ (400 $\text{MNm}^{-3/2}$) for the 7C specimen of the 62-ksi steel that was tested at +72 F.

Additional support for the conclusion that the K_c result for the 2T specimen is invalid can be seen from the fracture surfaces of the specimens tested at +72 F, Figure 11. Specifically, the nature of the stable crack extension for the 7C specimen was such that a "shear lip" (45-degree or 0.77 rad slant fracture) began to develop directly from the tip of the original fatigue crack at the specimen surface. A similar shear lip also began to develop for the 4T specimen but only after the original fatigue crack had extended on the expected crack plane by a small amount (1/8 to 1/4 inch, or 3.2 to 6.4 mm). However, the fracture surface for the 2T specimen was completely flat, without any evidence of stable shear-lip formation on the specimen surface prior to fracture. The fracture surface for the 2T specimen was the same as that obtained earlier for similar-size specimens tested in 3-point bending at the same +72 F temperature in attempts to measure static K_{Ic}.[10)] In both cases, the fracture surfaces were completely flat because of the constraining influence of the limited specimen ligament (W - a = 2.30 to 2.70 inches, or 58 to 69 mm), or specifically, the close proximity of the specimen back surface to the crack tip. Similarly, in both cases, the calculated K_{Ic} or K_c values (both calculated on the basis of LEFM) were invalid and exhibited substantial K_I-suppression effects.[10,13,14)] The K_{Ic} behavior and extent of K_I-suppression effects for the invalid K_Q results of both steels are discussed more fully below (Section 2F).

<u>1C. Effects of Temperature for B = 0.5-Inch Specimens</u>. The individual R-curves obtained for the B = 0.5-inch (12.7 mm) 2T and 4T specimens of the 50-ksi A572 Grade 50 steel tested at nominal temperatures of -40, +40, and +72 F are presented in Figures 12, 13, and 14, respectively. As with the earlier results for the B = 1.5-inch specimens, these results for the B = 0.5-inch 2T and 4T specimens are consistent in showing increasing amounts of stable crack extension preceding fracture, Δa_c, with increasing test temperature.

However, the corresponding variation in the K_c values with increasing temperature for the 2T and 4T specimens appears to be quite different, Figure 15. Specifically, the K_c values obtained with the 2T specimens appear to be insensitive to temperature, since all values were essentially in the range 300 ± 20 ksi $\sqrt{\text{inch}}$ (330 ± 22 $MNm^{-3/2}$). These results are in contrast to the results from the 4T specimens, which indicate a strong sensitivity to temperature, with the K_c behavior increasing from 150 ksi $\sqrt{\text{inch}}$ (165 $MNm^{-3/2}$) at -40 F (-40 C) to approximately 400 to 500 ksi $\sqrt{\text{inch}}$ (440 to 550 $MNm^{-3/2}$) at +72 F (+22 C). These different trends in behavior for the two different size specimens are reflected in the resulting fracture surfaces. In particular, all the 2T specimens tested show approximately the same amount of stable crack extension (Δa) on the actual fracture surfaces prior to fracture instability at K_c,

Figure 16, whereas the fracture surfaces of the 4T specimens show a corresponding marked sensitivity to temperature, Figure 17. The high degree of fracture toughness exhibited by the 4T specimens tested at +72 F can be seen in Figure 18.

1D. Nature of the Fracture-Instability Event. Except for three of the 24 specimens tested in the present study, all fractures occurred at K_c and in a catastrophic manner. Furthermore, this behavior was observed regardless of whether the tests were conducted under load-control or displacement-control conditions. The suddenness of the complete-fracture event at K_c may, at first, be somewhat unexpected for the tests conducted at the higher temperatures, particularly for those specimens tested under displacement-control conditions (maximum crack stability). However, such results are more easily understood when it is considered that this behavior is merely a reflection of the inherent strain-rate sensitivity (to fracture) for this steel, and therefore, for all steels of this same strength level (50 ksi or 345 MN/m^2), since strain-rate sensitivity of fracture behavior depends primarily on σ_{ys}.[10] Furthermore, this behavior is again less surprising when it is considered that even the toughest steels have limited ductility, and therefore fail in a similar sudden manner when tested in a conventional tension test.

The three exceptions to the behavior described above were all tested at +72 F (+22 C): the B = 1.5-inch 7C specimen and the duplicate B = 0.5-inch 4T specimens. This exceptional behavior occurred with the largest specimens tested at each thickness. The behavior obtained from these specimens with the larger in-plane dimensions is a more accurate measure of the intrinsic plane-stress crack tolerance for each thickness of A572 Grade 50 steel than the behavior obtained from the corresponding smaller specimens. Stated differently, the larger in-plane dimensions for these specimens allow measurements of the true R-curve to higher K_R levels before the results became biased because of violation of the presently undefined limits of COS validity. This reasoning leads to the obvious conclusion that the largest specimen size compatible with testing capabilities should be used in R-curve evaluations of high-toughness materials when it is evident that COS procedures are necessary.

As described previously, the reason that complete fracture did not occur for the B = 1.5-inch 7C specimen tested at +72 F was that the deflection limits of the displacement-control testing machine were exceeded. Thus, the K_c value for this 7C specimen was in excess of the K_R = 477 ksi $\sqrt{\text{inch}}$ (525 $\text{MNm}^{-3/2}$) value attained at test termination and, as discussed earlier, the inconsistent result obtained from the corresponding 2T specimen (apparent K_c = 87 ksi $\sqrt{\text{inch}}$ or 95 $\text{MNm}^{-3/2}$) can be dismissed as an invalid result occurring because of violation of COS requirements.

A similar type of influence can be seen in analysis of the $B = 0.5$-inch specimens tested at +72 F. These include the duplicate 4T specimens that exhibited exceptional behavior in not fracturing catastrophically at the cited K_c values. Specifically, these two 4T specimens yielded K_c values of >380 and >503 ksi $\sqrt{\text{inch}}$ (>420 and >550 $MNm^{-3/2}$), values of K_R that occurred at increments of stable crack extension, Δa, of 1.10 and 0.90 inches (28 and 23 mm), respectively, Figure 14. The extreme crack tolerance exhibited by these 4T specimens can be seen by the fact that complete catastrophic fracture occurred for each of these specimens <u>only</u> after significantly greater increments of stable crack extension, specifically, values of $\Delta a_c = 3.95$ and 3.47 inches (100 and 88 mm), respectively, Figure 17, and then <u>only</u> under the action of significantly higher crack-tip strain rates (intentional fracture). However, the above values were cited for K_c because subsequent calculations made for Δa values beyond 1.10 and 0.90 inches led to lower values of K_R, an unrealistic assessment of true plane-stress fracture behavior. Thus, although the true K_c values for the 4T specimens are clearly greater than the cited values of K_R, subsequent results for each of these specimens (because they are lower) again represent a clear violation of the presently undefined requirements for valid COS results. Such violations are not unexpected when it is considered that they occurred well beyond the attainment of the maximum load point (P_{max}), a value that represents limit-load or full-plastic-hinge conditions, Figure 19.

The above clear violation of COS requirements evident in the K_c results for the duplicate 4T specimens tested at +72 F indicates that there may be a similar influence in the specific K_c result obtained for the corresponding 2T specimen tested at +72 F (K_c = 308 ksi $\sqrt{\text{inch}}$ or 340 $MNm^{-3/2}$). The striking difference in the extent of the stable crack extension preceding fracture (Δa_c) evident on the fracture surfaces of these 2T and 4T specimens, Figures 16 and 17, would support this contention. Furthermore, the insensitive nature of the observed K_c values (300 ± 20 ksi $\sqrt{\text{inch}}$, or 330 ± 22 $MNm^{-3\ 2}$) over the entire temperature range from -40 to +72 F (-40 to +22 C), described earlier, is in sharp contrast to that expected on an intuitive basis and thus provides an additional indication of such a possibility. However, insufficient test results are available to indicate the extent to which the 2T specimen result may be influenced as a result of violation of COS requirements.

2. General Discussion

The influence of any parameter on the R-curve behavior of a given material can be measured in terms of any of the three principal characteristics of an R-curve: (1) the K_R value at the onset of stable crack growth, (2) the increment of stable crack extension at fracture instability, Δa_c, or (3) K_c. If the stable-crack-growth characteristics are neglected, the influence of any parameter on R-curve behavior can be reduced to a direct comparison of the resulting K_c values. It is on this basis that assessments of the influence of various parameters on R-curve behavior are described below.

<u>2A. Overall Scatter Observed in K_C Results.</u> When plane-stress fracture tests are conducted under fixed material and test conditions (T, $\dot{\varepsilon}$, and B) by using specimens with different initial crack lengths, a_o, some "scatter" in the resulting K_c behavior will occur. Specifically, K_c will increase with increasing crack length, a_o, for a well-behaved, homogeneous material ("K_c ordering"). Such behavior is, of course, the fundamental basis of R-curve characterization that was described in an earlier section of the present paper (see Figure 1). Such systematic variations in K_c with a_o are <u>not</u> real scatter at all, but rather the typical plane-stress fracture behavior that would normally be expected for any material. It is only the deviations from this systematic pattern of K_c-ordering behavior that can truly be referred to as scatter.

In the present work, the 2T, 4T, 4C, and 7C specimens tested had initial crack lengths, a_o, of nominally 1.75, 3.00, 3.45, and 5.80 inches (44, 76, 88, and 147 mm), respectively. Accordingly, the K_c value for a 7C specimen would be expected to be much higher than that for a 2T specimen (K_c ordering). Similarly, the K_c values for the 4T and 4C specimens would be expected to be intermediate between these extremes, with very little difference expected between the K_c values for the 4T and 4C specimens since the a_o values differ by only a small amount.

Deviations from this normal pattern of plane-stress fracture behavior (true scatter) can occur for a number of reasons. When more than one test method is used, as in the present work, the extent of such deviations from the normal K_c vs a_o behavior depends on (1) the repeatability of results from a single test method, (2) differences between test methods, and (3) variations in fracture toughness of the material tested.

The influence of each of these sources of true K_c scatter is described in subsequent sections relative to the summary of K_c results obtained for the B = 1.5-inch and B = 0.5-inch specimens, as given in Figures 8 and 15, respectively. However, prior to such analysis several comments are necessary. First, item 1 above involves both the repeatability of the testing conditions and the material variation. That is, items 1 and 3 are related and cannot be isolated entirely from each other. Second, the list given above does not include apparent K_c results obtained under conditions for which the basic stress analysis is violated, such as the violation of COS requirements described in a previous section, since such results represent an artifact and not true K_c scatter.

2B. Repeatability of K_c Results for a Specific Test Method. The repeatability of K_c results, or the lack thereof, can only be measured by a direct comparison of individual test results obtained under the same conditions of specimen size, test temperature, and test technique (load-control or displacement-control techniques). If only duplicate specimen tests are available for such purposes, as in the present study, conclusions based on such a small number of results <u>must clearly involve reservations</u>. However, no alternative choice exists for making an assessment of repeatability in the limited results of the present study on A572 Grade 50 steel.

Four different sets of duplicate specimen tests are available for such assessments in the present study. In particular, Table VI shows that the variations in the average K_c values obtained from duplicate 2T, 4T, 4C, and 7C specimens are ±7, ±14, ±12, and ±29 percent, respectively. These variations <u>cannot</u> be related to systematic changes in specimen size because the concomitant test conditions (thickness and test temperature) for each specimen type were different, Table VI. The results in Table VI suggest that singular K_c variations of less than ±30 percent relative to the average K_c value obtained for duplicate specimens of A572 Grade 50 steel would be expected for tests conducted using either the load-control or the displacement-control testing techniques.

By comparison, the variation in K_{Ic} values for specially melted high-strength steels exhibiting good homogeneity, such as 18Ni(250 Grade) maraging steels, has been shown earlier to be within ±5 or ±10 percent, depending on the total number of specimens used and the participating laboratories.[15,16] Furthermore, the variation in K_{Ic} values for lower strength steels exhibiting both less homogeneity and a K_{Ic} transition behavior has been shown to be as large as ±25 percent or more for a given temperature and strain rate.[10,14,17,18,19,20] Thus, the presently observed variation of as much as ±29 percent in one case for the K_c behavior of A572 Grade 50 steel, a similar low-strength steel, is not surprising. That is, despite the different fracture modes (K_c vs K_{Ic}), the present variation in results (K_c repeatability) appears to be no greater than that (K_{Ic} repeatability) observed earlier in similar low-strength steels.

2C. Load-Control vs Displacement-Control Test Methods. To assess the influence of the testing procedure (load-control vs displacement-control test methods) on the K_c values obtained, it is necessary to compare specific results obtained with each procedure for specimens of the same size (that is, with the same W and B dimensions). Results from the same size specimen for both test procedures are necessary in order to exclude any additional influence of crack length, a_o, on the K_c value.

Such a basis of comparison is available from the results of the 4T specimens tested under load-control conditions and the 4C specimens tested under displacement-control conditions, listed as items No. 4 through 10 in Table V. The minimal difference in the initial crack lengths, a_o, for the 4T (a_o = 3.00 inches) and 4C specimens (a_o = 3.45 inches) can be discounted as second-order effects in such comparisons. A comparison of the K_c values for the 4T and 4C specimens is given in Table VII. These limited results show that there is a definite influence of the test procedure. In particular, the 4T specimens tested under load-control conditions at nominal temperatures of -40, +40, and +72 F exhibited K_c values that were higher than the corresponding K_c values obtained under displacement-control conditions by 51, 80, and 40 percent, respectively. Although such direct comparisons are admittedly limited in number, they do nevertheless provide a consistent behavior. That is, these results indicate that the K_c value obtained with the load-control procedure is, on the average, 57 percent higher (1.57 factor) than that for the same size specimen tested using the displacement-control procedure. Furthermore, the higher K_c values for the 4T specimens tested under load-control conditions are considerably in excess of the maximum observed variation of ±29 percent that might be expected strictly on the basis of repeatability (as discussed in the previous section).

While this influence of testing method on the K_c result appears to be real, it cannot be fully verified using statistical analysis procedures. That is, the present results on K_c repeatability (previous section) cannot be used to meaningfully assess the standard deviation (σ) for the variability in K_c because both the basic nature of the variability cannot be accurately ascertained* and the total number of duplicate tests (4 sets) available are insufficient in number. The standard deviation for the variability in K_c must be

---

* Statistical tests to determine the fundamental character of the present variability in K_c values are inconclusive. That is, it is not known with confidence if the variation is constant (in absolute terms) and independent of K_c level, or whether the variation is proportional to the mean K_c level.

known accurately before confidence levels (67 percent for $\pm\sigma$ and 95 percent for $\pm 2\sigma$) can be established in relation to the statistical assessment of the influence of testing procedure on K_c.

However, careful inspection of all the K_c results for the B = 1.5-inch specimens in Figure 8 also reinforces the basic conclusion that there is an influence of the test procedure. In particular, the K_c values obtained for the 2T and 4T specimens tested under load-control conditions generally fall in the upper half of the "scatter" band, whereas the K_c values for the 4C and 7C specimens tested under displacement-control conditions generally fall in the bottom half of the scatter band.

The specific cause of the consistent differences between the K_c values obtained with the load-control and displacement-control techniques is unknown. Furthermore, such differences were unexpected and in sharp contrast to the earlier results by Heyer and McCabe[9)] which demonstrated complete equivalence between the two loading techniques for both high-strength aluminum and titanium alloys. Specifically, these earlier results showed, for each of a range of eight (8) different material conditions, that K_c values determined directly with the load-control technique differed by less than ±5 percent from the corresponding K_c values determined with the displacement-control technique.

These earlier results of Heyer and McCabe were all obtained on nonferrous materials in thin sheet form (B = 0.066 inch or

1.7 mm or less); the fracture properties (K_c) of the sheet are quite reproducible and primarily independent of strain rate, so that the results were analyzed under completely LEFM conditions. In contrast, the present results on A572 Grade 50 steel are from thick plate (B = 1.5 inches); the fracture properties (K_c) of the plate are of questionable reproducibility (see previous and subsequent sections) and highly dependent on strain rate (as indicated by earlier K_{Ic} behaviors), and the fracture toughness (K_c) is so high, that the results must be analyzed under COS conditions. These five (5) primary differences between the earlier studies of Heyer and McCabe and the present studies are summarized in Table VIII. Such differences in testing conditions can be combined with consideration of strain-hardening characteristics to provide a salient starting point for the future research work that is necessary in order to understand the reasons for the differences observed in the present K_c results on A572 Grade 50 steel as determined by the load-control and displacement-control techniques.

2D. Effects of Thickness (B = 1.5 inch vs B = 0.5 inch) for the Load-Control Test Method.

Because the previous section showed that the K_c results are influenced by testing method (load control vs displacement control) an assessment of the influence of specimen thickness (B = 1.5 inch vs B = 0.5 inch) can only be made in a meaningful manner using a single test method. Such comparisons are available from the load-control tests conducted using both 2T and 4T specimens for each of the B = 1.5-inch and B = 0.5-inch thicknesses. The results from these direct comparison tests are summarized at each of the three different test temperatures in Table IX.

The specific results for the 2T specimens in Table IX show that there is an effect of thickness, with higher K_c values consistently being obtained for the thinner (B = 0.5 inch) specimens than those for the thicker (B = 1.5 inch) specimens. This result is consistent with expectations based on both R-curve philosophy and plane-stress fracture behavior generally. However, the results for the 4T specimens in Table IX do not support this contention. That is, these 4T specimen results show that there is no effect of specimen thickness on K_c behavior. Accordingly, these results on the effects of specimen thickness relative to K_c behavior are inconclusive.

The lack of a consistent trend relative to the influence of thickness on K_c behavior is apparently related to the local variations in fracture toughness for the 50-ksi A572 Grade 50 steel. That is, the local variations in fracture toughness are apparently of greater consequence in relation to K_c than are the resulting differences in behavior between the B = 1.5-inch and B = 0.5-inch-thickness specimens. Thus, the local variation in fracture toughness for the 50-ksi A572 Grade 50 steel presently tested is apparently large enough to mask the true effect of specimen thickness on K_c behavior.

<u>2E. Local Variation in Fracture Toughness</u>. The discussion in section 2A describes the normal, expected plane-stress fracture behavior (K_c increasing with increasing a_o). The discussions in sections 2B and 2C indicate that real scatter in K_c values (or

true deviations from the expected systematic behavior) can be caused by the repeatability of a given test procedure or by differences between the load-control and displacement-control test procedures, or by both. Further deviations from the normal dependence of K_c on crack length, a_o, can also be caused by local variation in the fracture toughness of the material.

The summary of the present K_c results given in Figures 8 and 15 shows that when each of the two test procedures used is considered separately, the normal K_c behavior was usually observed, except for the results discussed below. That is, at each of the -40 F, +40 F, and +72 F test temperatures, the K_c values obtained for the 4T specimens were, as expected, higher than the corresponding K_c values for the 2T specimens for those tests conducted with the load-control procedure. Likewise, the K_c results for the 7C specimens were higher than the corresponding values for the 4C specimens for the tests conducted with the displacement-control procedure.

Exceptions to this normal K_c behavior occurred with each of the test procedures at -40 F, Table V. Specifically, for the B = 1.5-inch plate tests conducted with the displacement-control procedure, Figure 8 shows that a higher K_c value occurred for the 4C specimen (K_c = 102 ksi $\sqrt{\text{inch}}$ or 112 $\text{MNm}^{-3/2}$) than for the 7C specimen (K_c = 57 ksi $\sqrt{\text{inch}}$ or 63 $\text{MNm}^{-3/2}$). Similarly, for the B = 0.5-inch plate tests conducted with the load-control procedure, Figure 15 shows that a higher K_c value occurred for the 2T specimen

(K_c = 316 ksi $\sqrt{\text{inch}}$ or 348 $MNm^{-3/2}$) than for the 4T specimen (K_c = 150 ksi $\sqrt{\text{inch}}$ or 165 $MNm^{-3/2}$). That is, for each test procedure at the -40 F temperature, a higher K_c value would normally be expected for the larger specimen (because of the larger initial crack length, a_o), whereas a lower K_c value was actually obtained. These anomalous results—that is, these two inversions in the expected behavior—represent real K_c scatter and may be related to local variations in the fracture toughness of the A572 Grade 50 steel tested.

Another measure of local variation in the fracture toughness of the material may be obtained from Charpy V-notch (CVN) test results. Consequently, a number of CVN specimens were obtained directly from a select number of the CT specimens used in the R-curve tests. All CVN specimens were taken as close as possible to the original fracture surface of the corresponding CT specimens and in such a manner that the notch orientation for each of the CVN specimens was identical to that for the CT specimens. Approximately 10 CVN specimens were prepared from each of 11 CT specimens and tested at +72, +40, 0, and -40 F (+22, +4.5, -18, and -40 C).

The results of the CVN tests are presented in Table X, along with the results for the corresponding CT specimens. The CVN data were obtained to establish some measure of local variation of fracture toughness rather than to establish correlation between K_c and CVN test results. Because of differences in notch acuity, strain rate, and state-of-stress, any such correlations are fortuitous.

However, the variations in local fracture toughness, as measured by testing CVN specimens, can be seen when all the CVN energy-absorption values are plotted as a function of test temperature, Figure 20. The ratios of the maximum to the minimum CVN values observed at -40, +40, and +72 F (K_c test temperatures) were 7:1, 3:1, and 2.5:1, respectively. Thus, these CVN energy-absorption values, which are not at all untypical for A572 Grade 50 steel, show a large degree of variation at the same -40 F test temperature at which the anomalous K_c results were obtained. That is, the CVN results would appear to confirm that local variations in the fracture toughness of the 50-ksi A572 Grade 50 steel tested may be responsible for the inverted K_c behaviors obtained at -40 F.

Local variations in the fracture toughness of the A572 Grade 50 steel tested can also be assessed in terms of a ductility criterion rather than an energy-absorption criterion. To illustrate, when the CVN lateral-expansion (LE) values for this A572 Grade 50 steel were plotted against the corresponding CVN energy-absorption values, the correlation was nearly 1:1, as shown in Figure 21. It can therefore be concluded that a similar large variation in fracture ductility, as measured by the LE values, occurs at the -40, +40, and +72 F test temperatures.

2F. Comparison of K_C and K_{IC} Behaviors. The variation of plane-strain fracture toughness, K_{Ic}, with temperature for the present A572 Grade 50 steels has been documented in a previous study.[10] For reference, the static K_{Ic} results of both the 50-ksi and 62-ksi steels are presented in Figures 22 and 23, respectively. These figures show that valid K_{Ic} measurements could not be made above K_{Ic} = 55 ksi $\sqrt{\text{inch}}$ (60 $MNm^{-3/2}$) for either of the A572 Grade 50 steels. In particular, this level of K_{Ic} (measured at the $\beta = 0.40$ line intersection) occurred at -160 F (-107 C) for the 50-ksi steel and at -60 F (-51 C) for the 62-ksi steel. For each steel, this K_{Ic} measurement limitation was a direct result of the limited plate thickness available (B = 1.5 inches). Attempts to extrapolate K_{Ic} behavior to higher K_I values and temperatures well beyond β = 0.40 may lead to erroneous conclusions, particularly when, as for the present steels, only a small portion of the K_{Ic} transition has been established. The inability to measure static K_{Ic} values at the higher temperatures (-40 to +72 F) was, of course, the primary reason for the present R-curve studies in this higher temperature range.

The K_c results for the B = 0.5-inch CT specimens of the 50-ksi steel obtained at temperatures between -40 and +72 F are consistent with the corresponding valid K_{Ic} test results, Figure 22. That is, these results represent typical fracture behavior with $K_c > K_{Ic}$ at a given temperature as would be expected because of the different states of stress. Specifically, the K_c values of 150 ksi $\sqrt{\text{inch}}$ (165 $MNm^{-3/2}$) and higher determined experimentally for the B = 0.5-inch CT specimens at -40 F and above are in excess of the corresponding K_{Ic} values that would be estimated at the same temperatures by direct extrapolation of the valid K_{Ic} results at cryogenic temperatures.

Several observations can be made when the present K_c results for the B = 1.5-inch CT specimens of both the 50-ksi and 62-ksi A572 Grade 50 steels are compared with the earlier valid K_{Ic} results on the same scale, Figure 24. First, the two K_c results for the 62-ksi steel (K_c = 121 ksi $\sqrt{\text{inch}}$ at -40 F and K_c = 365 ksi $\sqrt{\text{inch}}$ at +72 F) are again completely consistent with normal expectations. That is, these K_c values are each higher than the corresponding K_{Ic} estimates of behavior that would result from direct extrapolation of the valid K_{Ic} results at cryogenic temperatures for this A572 Grade 50 steel (i.e., typical plane-strain/plane-stress fracture behavior at a given temperature). Second, the present K_c results for the B = 1.5-inch CT specimens of the 50-ksi steel would appear to be somewhat inconsistent with corresponding estimates of K_{Ic} behavior obtained by direct extrapolation to the -40 to +72 F temperature range. That is, the experimentally observed K_c values would appear to be lower than the estimated K_{Ic} values expected from the extrapolation procedure. This apparent inconsistency remains to be explained.

If the K_c results obtained under load-control conditions (2T and 4T specimens) are considered alone, an apparent discrepancy still exists relative to the K_{Ic} behavior. However, the extent of such a discrepancy is far less under such circumstances than is the case when all the B = 1.5-inch CT results, including the K_c results obtained under displacement-control conditions (4C and 7C specimens), are considered simultaneously. As described in a previous section, the reasons for the differences between the K_c values resulting from the load-control and displacement-control testing methods are unknown and further complicate attempts to show compatibility of the present K_c and earlier K_{Ic} behaviors.

The apparent inconsistency between the K_{Ic} and K_c behaviors for the B = 1.5-inch specimens of the 50-ksi steel can be described in terms of the corresponding transition temperatures. That is, Figure 22 shows that the K_{Ic} transition temperature is -160 F (-107 C), with the K_{Ic} value increasing abruptly from 30 to 60 ksi $\sqrt{\text{inch}}$ in this temperature region. Similarly, Figure 24 shows that the K_c transition temperature for B = 1.5-inch plate is approximately 0 F, with the <u>minimum</u> K_c value increasing abruptly from 100 ksi $\sqrt{\text{inch}}$ at 0 F to 300 ksi $\sqrt{\text{inch}}$ at +72 F. These results show conclusively that both the K_{Ic} and K_c transitions (1) are quite steep, (2) occur at different temperatures, and (3) represent two entirely different levels of crack tolerance; the K_c transition, unlike the K_{Ic} transition, represents unstable crack extension preceded by significant stable crack propagation (Δa) which was as high as 4 inches.

The apparent inconsistency between the current K_c transition for the B = 1.5-inch plate of the 50-ksi steel and the corresponding K_{Ic} transition may be explained if it can be established that a K_{Ic} shelf behavior exists, as shown schematically in Figure 25. The existence of a K_{Ic} shelf behavior has been established earlier in 100-ksi-strength steel that is susceptible to temper embrittlement.[19)] Support for the possible existence of such a behavior in the 50-ksi A572 Grade 50 steel investigated may be obtained from three different sources: (1) J-integral concepts,[21,22)] (2) principles of the K_I-suppression effect,[13)] and (3) CVN specimen results.

The nonlinear concepts of fracture behavior offered by the J-integral and K_I-suppression concepts are necessary since the alleged K_{Ic} shelf behavior appears to occur well above that level which can be measured validly under LEFM conditions with the B = 1.5-inch plate available (K_{Ic} = 55 ksi $\sqrt{\text{inch}}$ at β = 0.40 intersection, Figure 22). These nonlinear concepts have been used to reanalyze the earlier invalid K_{Ic} results which exhibit increasingly more severe K_I-suppression effects for increasing temperatures above -120 F (-85 C), Figure 22. In summary form, reanalysis of the 3-point bend tests conducted at -120 and +72 F using J-integral concepts, on a conservative basis, indicated J_{Ic} values that correspond to K_{Ic} values of 130 and 200 ksi $\sqrt{\text{inch}}$ (143 and 220 $MNm^{-3/2}$), respectively. When cognizance is taken of the fact that the $(\frac{a}{W})$ value in these tests was 0.50 instead of the near optimum 0.80 normally suggested for J-integral tests (a condition that would lead to values that are optimistic by about 20%), the adjusted K_{Ic} values at -120 and +72 F are approximately 100 and 160 ksi $\sqrt{\text{inch}}$ (110 and 176 $MNm^{-3/2}$), respectively. These conservative J-integral calculations indicate a gradual increase in K_{Ic} with temperatures above -120 F, essentially a K_{Ic} shelf behavior, rather than continuation of the steep K_{Ic} transition established for lower K_I values at -160 F.

Reanalysis of the same invalid K_{Ic} results using K_I-suppression effect concepts, described in detail elsewhere,[13] lends additional support to the possible existence of a K_{Ic} shelf behavior. In particular, it has been shown earlier[13] on a 70-ksi yield-strength steel that the apparent K_Q value is suppressed to a value of 1/2 the true K_{Ic} value when $\left(\frac{K_Q}{K_{I,Gub}}\right) = 1.00$, a condition which occurs when the test-specimen dimensions (W, B, and a) are only 1/10 of those required for a valid K_{Ic} result under LEFM conditions. Table XI shows that this condition of $\left(\frac{K_Q}{K_{I,Gub}}\right) = 1.00$ would occur at approximately -80 F (-62 C) and that the corresponding "corrected" or true K_{Ic} value would be about 148 ksi $\sqrt{\text{inch}}$ (163 $MNm^{-3/2}$)--the correction being achieved by multiplying the observed K_Q value of 74 ksi $\sqrt{\text{inch}}$ by a factor of 2.0. Furthermore, because the $\left(\frac{K_Q}{K_{I,Gub}}\right)$ ratio for all the invalid K_{Ic} tests is approximately the same (increasing only gradually from 0.94 at -120 F to approximately 1.10 or so at +72 F), these K_I-suppression effect results complement the J-integral results in providing strong indications that a K_{Ic} shelf behavior occurs for the 50-ksi yield-strength A572 Grade 50 steel over the temperature range -120 to +72 F. These estimated K_{Ic} behaviors obtained from both the K_I-suppression effect and J-integral concepts are summarized in Table XII.

Additional evidence in support of the K_{Ic} shelf behavior but of a less direct nature can be seen from the results of CVN specimen tests. Specifically, Figure 26 shows that whereas the concept of a double shelf or double transition in the CVN energy-absorption behavior is only marginally observable under dynamic loading conditions ($\dot{\varepsilon} \cong 10^{+1}$ sec^{-1}), such behavior is clear and unmistakable under the same static loading conditions ($\dot{\varepsilon} \cong 10^{-5}$ to 10^{-4} sec^{-1}) used for the present K_c tests. Although these results are presented in terms of an energy criterion, the same double-shelf or double-transition behavior can also be seen in terms of a ductility criterion, Figure 27, and, are further confirmed by considerations of fracture appearance (percent shear) behavior as well. These latter considerations also verify the existence of the upper shelf at temperatures of +30 F and higher (100% shear behavior) for the statically-tested specimens in Figures 26 and 27.

The present investigation represents the only currently known attempt to simultaneously evaluate both the K_{Ic} and K_c behaviors of an intermediate-strength structural steel in a comprehensive manner. The preceding results from analysis by J-integral and K_I-suppression effect concepts as well as the quantitative CVN test results are all consistent in indicating the possible existence of a K_{Ic} shelf behavior (slight positive slope) for the 50-ksi yield-strength A572 Grade 50 steel. Such behavior would clearly resolve the apparent anomaly between the present K_c transition for the B = 1.5-inch plate and the lower temperature K_{Ic} transition behavior found earlier. While such a K_{Ic} shelf behavior has not been established beyond question, it is a consistent result from state-of-the-art application of nonlinear analysis techniques that are still undergoing intensive development. Because specimen thicknesses from B = 10 to 25 inches would be required to establish the K_{Ic} shelf behavior under valid LEFM conditions (valid K_{Ic}), it is clear that positive verification must await specifically designed tests conducted with subsize specimens and similar, but more refined, nonlinear analysis techniques in the future.

2G. Reservations Concerning Present R-Curve Results. Descriptions of present specimen behavior above have indicated that the initial, stable crack extension for high levels of fracture resistance was such that a shear lip started to form directly from the tip of the original fatigue crack at the specimen surface, as illustrated in Figures 11, 17, and 18. That is, in the early stages of stable crack extension, the crack at the specimen surface is inclined at some angle, θ, relative to the anticipated, flat crack-extension plane. In a later stage of stable crack extension, a full-slant fracture will develop through the specimen thickness (B) with a resulting crack plane that is oriented at an angle of 45 degrees (0.785 rad) to the anticipated, flat crack-extension plane.

While these two different types of deviation from a flat crack-extension plane are typical for any material under true plane-stress conditions, their existence introduces additional complexities into the analysis. Specifically, a flat crack plane that is perpendicular to the applied stress (σ) corresponds to the most common type of mode I deformation of the crack, characterized by the K_I parameter. Deviations from such a flat crack plane introduce additional mode II and III deformation of the crack, described by the corresponding stress-intensity components K_{II} and K_{III}.

In all R-curve and K_c studies, including the present investigation, mode I deformation of the crack is dominant and is the only one considered in the analysis (K calculations). Such consideration of mode I alone persists even when additional mode II and III deformation components may also occur as a result of deviations from a flat crack plane. The influence of such additional modes of loading on the K_c value (calculated on the basis of mode I alone) is currently unknown. This unknown influence forms the basis of the reservations extended in relation to the accuracy of the present K_c values, particularly those for $K_c \geq 150$ to 200 ksi $\sqrt{\text{inch}}$ (165 to 220 $\text{MNm}^{-3/2}$) which required analysis by the COS method. However, as can be seen from the next section of this paper, the concern over the precision of such high K_c levels for a σ_{ys} = 50-ksi steel is more of an academic rather than practical nature. That is, once a behavior corresponding to a $\left(\frac{K_c}{\sigma_{ys}}\right)$ between 2.0 and 3.0 is achieved, extensive crack tolerance (a_{cr}) is automatically guaranteed under applied elastic stress levels ($\sigma_D \leq \sigma_{ys}$).

3. Significance of Present R-Curve Results

3A. Critical-Flaw-Size Calculations. The significance of K_{Ic} values and K_c values derived for a given crack length (a) from a single R-curve has been discussed in concept earlier.[20] For such determinations, the parameter of ultimate interest is the critical flaw size (a_{cr}) required to cause fracture instability under the same material and test conditions (T, $\dot{\varepsilon}$, and B) used to measure the specific K_{Ic} or K_c value. The specific a_{cr} value is further related to the level of the design stress, σ_D, relative to σ_{ys} for a given specimen or structural geometry. A normalized plot showing the general relationship of a_{cr} to such parameters for a large center-cracked tension (CCT) specimen subjected to uniform tension is presented in Figure 28. Because of the normalized basis of the plot, Figure 28 can be used to calculate a_{cr} values for a CCT specimen of any material ($\therefore \sigma_{ys}$) for which valid fracture-mechanics results (K_{Ic}, K_{Id}, K_c, K_{Iscc}) are available under the loading rate, temperature, and state-of-stress of interest.

The specific K_c results of the current study have been summarized earlier in Figures 8 and 15. The minimum values corresponding to the bottom of the K_c scatter band for each set of results in Figures 8 and 15 can be translated into corresponding minimum values of a_{cr} for a CCT specimen with the aid of Figure 28. On the basis of the test results obtained in this study, it can be shown, Table XIII, that the minimum values of a_{cr} for 1.5-inch-thick CCT specimens subjected to a design stress, σ_D, equal to 3/4 the yield strength, σ_{ys}, are 0.58, 5.22, and 22.9 inches (14.7, 133, and 580 mm) at -40, +40, and +72 F, respectively. Table XIII also shows that at the same -40, +40, and +72 F temperatures and for the same ratio of σ_D/σ_{ys}, the minimum values of a_{cr} for B = 0.5-inch

CCT specimens are 4.06, 16.2, and >32.7 inches (103, 410, and >830 mm), respectively.

Because of the nature of the calculation for a CCT specimen, the a_{cr} value represents only half of the total central crack length. That is, the total critical crack length for a CCT specimen is $2a_{cr}$. When this is taken into account, the above results show with one exception that the total critical crack length ($2a_{cr}$) corresponding to the minimum fracture behavior for each of the different combinations of plate thickness (B) and test temperature is at least 7 times the plate thickness ($2a_{cr} \geq 7B$).

The single exception is for the B = 1.5-inch plate at -40 F, for which the total critical crack length is on the same order as the plate thickness ($2a_{cr}$ = 1.16 inches or 29.5 mm $\cong$ B). However, this calculation is based on a single data point (K_c = 57 ksi $\sqrt{\text{inch}}$ or 63 $MNm^{-3/2}$ for a 7C specimen) of doubtful representation, as discussed earlier. That is, if a more representative minimum behavior for this condition is on the order of K_c = 100 ksi $\sqrt{\text{inch}}$ (110 $MNm^{-3/2}$), as was indicated by a duplicate specimen test (K_c = 103 ksi $\sqrt{\text{inch}}$ or 113 $MNm^{-3/2}$ for a 7C specimen at -40 F, Table V), the corresponding a_{cr} value in Table XIII would be 1.80 inches (46 mm). In such a case the associated total critical crack length would be on the order of two and a half times plate thickness ($2a_{cr}$ = 3.6 inches or 91 mm $\cong$ 2.5B). However, an insufficient number of tests were conducted in the present study to assess the most typical behavior on a statistical basis.

The above a_{cr} values are based on using a criterion of $\sigma_D = 3/4\ \sigma_{ys}$ for the minimum K_c behavior, Table XIII. If calculations of a_{cr} are desired on the basis of a different σ_D criterion for the same minimum K_c behavior, they may be obtained quickly with the use of Figure 28. This same figure can also be used to obtain similar a_{cr} results for the median or maximum K_c behavior by using the corresponding center and top portions of the scatter bands shown in Figures 8 and 15.

3B. Application of Results to Structures. The a_{cr} values cited in the previous section are applicable to structures in direct proportion to the extent that the assumptions used in the basic calculation are satisfied. That is, the cited a_{cr} values are directly applicable for a structural configuration in which plane-stress conditions exist and the conditions of a large CCT specimen subjected to a remotely applied uniform stress (σ_D) equal to 3/4 the yield strength are approximated. While differences in the nature of the stress (bending as opposed to tension) can be handled analytically,[23,24] the requirements of plane-stress conditions and large planar dimensions for the structural component are mandatory.

An example of the applicability of the a_{cr} values can be given in terms of a typical structural member, such as a large H-beam (girder) with typical thicknesses for both the flange and the web on the order of 1/2 to 1-1/2 inches. Specifically, the

a_{cr} values cited would have application for through-thickness cracks located in the web of such a beam, where plane-stress conditions would exist. However, the same a_{cr} values would have no application for partial-thickness cracks (PTC) emanating from the top surface of the tension flange of the beam (such as would occur at the base of a cover plate due to fatigue), since the stress state at this location is primarily one of plane strain.

These same stress-state (plane stress) and structural (large planar dimensions) requirements are necessary for the interpretation of essentially <u>all</u> R-curve measurements, since such measurements intrinsically deal with materials exhibiting high levels of crack tolerance. In turn, high levels of crack tolerance under plane-stress conditions imply the existence of either very large critical flaws (a_{cr}) under low levels of elastic stress ($\sigma_D \leqq 1/2\ \sigma_{ys}$), Figure 28, or high K_c levels that translate, for short cracks (a), into large values of the corresponding critical crack-tip plastic zone, r_p, under the action of high elastic stress ($1/2\ \sigma_{ys} \leqq \sigma_D \leqq \sigma_{ys}$). In either case, <u>containment</u> of such values within a large elastic-stress field is <u>necessary</u> before a_{cr} calculations can be valid (a fundamental principle of LEFM). Accordingly, to accomplish this containment for plane-stress conditions, large planar dimensions relative to the thickness, B, are necessary for either a specimen or a structural element.

The useful life of an H-beam subjected to load fluctuations is essentially completed when a PTC crack on the tension surface penetrates partially through the flange. As described above, the stress state for cracks located in this tension-flange region is essentially one of plane strain—whether it is analyzable in terms of current LEFM concepts (K_{Ic}) or not. Consequently, measurements of plane-stress fracture resistance, such as obtained with either R-curve or direct K_c measurements, have no meaning in relation to the useful life or the load-carrying capacity of such a beam.

Such plane-stress measurements would only have application in predicting the a_{cr} value at which catastrophic fracture of the H-beam would occur. For all the conditions investigated in the present study, complete failure of this type would occur only after the crack (1) had penetrated completely through the tension flange by fatigue, and (2) had subsequently propagated into the web to a crack length many times the web thickness ($a_{cr} >> B$). However, since the useful structural life of such an H-beam is expended after the first stage of fatigue-crack propagation (a condition requiring perhaps 40 to 50 years in most structural applications such as bridges), and either the H-beam is replaced or the entire structure retired from service at this point, it is academic to conjecture about the possible nature of a catastrophic fracture event that will not occur. However, the level of confidence that such an event will not occur in service can be measured in terms of the extent to which $a_{cr} > B$, when the appropriate material and test conditions (T, $\dot{\varepsilon}$, and B) have been taken into account. It is in

STP591-EB/Feb. 1976

this indirect sense of assessing structural integrity that measurements of plane-stress fracture resistance (R-curve and K_c measurements) can be beneficial when applied to structural components in service.

Summary and Conclusions

Specific R-curve results were obtained on two different heats of ASTM A572 Grade 50 steel over the temperature range -40 to +72 F (-40 to +22 C) by using a total of 24 CT specimens. Of this total, 14 specimens had in-plane dimensions corresponding to 2T and 4T specimens and were tested under load-control conditions; the remaining 10 specimens had in-plane dimensions corresponding to 4C and 7C specimens and were tested under displacement-control conditions. Twenty-two (22) of the specimens tested were of a 50-ksi yield-strength A572 Grade 50 steel, and the two (2) remaining specimens were of a 62-ksi yield-strength A572 Grade 50 steel. Both 1.5-inch-thick and 0.5-inch-thick (38 and 12.7 mm) specimens were evaluated from the 50-ksi steel; the two specimens of the 62-ksi steel were both 1.5 inches thick. All specimens were tested under static loading conditions ($\dot{\varepsilon} \cong 10^{-5}$ sec^{-1}). The current study represents the first known attempt to evaluate the R-curve behavior of a high-strength structural steel. The specific results obtained from this pioneer study can be summarized as follows:

1. A steep transition was observed in the plane-stress fracture behavior for the B = 1.5-inch specimens of the 50-ksi steel, with <u>minimum</u> K_c values of 57, 155, and 318 ksi $\sqrt{\text{inch}}$ (63,

171, and 350 $MNm^{-3/2}$) occurring at temperatures of -40, +40, and +72 F (-40, +4.5, and +22 C), respectively.

2. No significant differences were observed in the K_c behavior of the 50-ksi and 62-ksi A572 Grade 50 steels.

3. Greater overall resistance to fracture was observed for the B = 0.5-inch specimens than for the B = 1.5-inch specimens of the 50-ksi steel, with <u>minimum</u> K_c values of 150, 273, and >380 ksi $\sqrt{\text{inch}}$ (165, 300, and >418 $MNm^{-3/2}$) occurring at temperatures of -40, +40, and +72 F, respectively. However, this difference in the minimum resistance to fracture for the 0.5- and 1.5-inch-thick specimens is partially the result of differences due to testing method (see conclusions 6 and 7).

4. With the exception of three specimens, the fracture instability for all specimens was catastrophic in nature. The excepted specimens, all tested at +72 F, included a 7C specimen with B = 1.5 inches that exceeded testing-machine capacity at K_R = 477 ksi $\sqrt{\text{inch}}$ (525 $MNm^{-3/2}$) and Δa = 0.86 inch (22 mm), and duplicate 4T specimens that exhibited slow, stable crack extension corresponding to $\Delta a_c \geq$ 3.50 inches ($\geq$ 90 mm) at K_c values of >380 and >503 ksi $\sqrt{\text{inch}}$ (418 and 550 $MNm^{-3/2}$).

5. The repeatability of results for three of four sets of duplicate specimens was within ±15 percent of the average K_c value measured. The repeatability of results for the fourth set of specimens was within ±30 percent of the average K_c value measured.

6. The choice of testing procedure (load-control vs displacement-control) was found to influence the results. The K_c values for the 4T specimens tested under load-control conditions were 40 to 80 percent higher than the values for the corresponding 4C specimens tested under displacement-control conditions in direct comparison tests at three different temperatures. This influence of testing procedure was consistent and appears real, but could not be fully verified using statistical analysis procedures.

7. The effects of specimen thickness (B = 1.5 inch vs B = 0.5 inch) on K_c behavior evaluated in direct comparison tests using only the load-control testing procedure were inconclusive. Results from 2T specimens tested at three different temperatures indicated a consistent influence, while results from 4T specimens tested at similar temperatures were consistent in indicating no influence. Local variations in fracture toughness were apparently large enough to mask the true effects of specimen thickness on K_c behavior.

8. In relation to effects of specimen size, normal plane-stress fracture behavior (increasing K_c values corresponding to increasing values of a_o) was generally obtained with both the load-control and the displacement-control testing methods at all temperatures. However, an inversion in this behavior occurred with each test method at -40 F (-40 C). These departures from expected behavior may be related to inherent variations in the local fracture toughness.

9. The K_c results of the present study were shown to be consistent with earlier K_{Ic} results obtained from tests on the same steel at cryogenic temperatures. The central concept in resolving obvious differences in the corresponding K_c- and K_{Ic}-transition temperatures was the apparent existence of an intermediate K_{Ic} shelf, a behavior supported by the results of each of three different and entirely independent methods of analysis (J-integral K_I-suppression effect and CVN specimen results).

10. For normal stress levels used in design ($\sigma_D = 3/4\ \sigma_{ys}$), critical flaw sizes ($a_{cr}$) for the B = 1.5-inch plate of the 50-ksi A572 Grade 50 steel were shown to be a_{cr} = 1.80, 5.2, and 23.0 inches (46, 132, and 585 mm) for <u>minimum</u> representative behavior at -40, +40, and +72 F, respectively.

11. For normal stress levels used in design, the critical flaw sizes for the B = 0.5-inch plate of the 50-ksi A572 Grade 50 steel were shown to be a_{cr} = 4.0, 16.0, and >32.0 inches (100, 400, and >800 mm) for <u>minimum</u> representative behavior at -40, +40, and +72 F, respectively.

12. With two exceptions, the total critical flaw size ($2a_{cr}$) for cracks centrally located in a large plate subjected to uniform tension stress were shown to be in excess of seven times the plate thickness, ($2a_{cr} \geqq 7B$) for all the 8 different combinations of plate thickness and temperature investigated for the A572 Grade 50 steels.

13. Values of a_{cr} calculated from measurements of plane-stress fracture resistance (R-curve and K_c measurements) can be applied validly only when the state of stress in the structural application is plane stress, and then only under the assigned material and test conditions (T, $\dot{\varepsilon}$, and B). Accordingly, such values would be directly applicable to structures with large planar dimensions (direction of crack propagation), including the web location for large H-beams. Such a_{cr} values would not be directly applicable in confined structural regions, such as in the tension-flange region of H-beams (complete inapplicability) and the web region of H-beams with small web dimensions (indirect applicability of a_{cr} values for assessing the confidence level of structural integrity).

Many of the results above were obtained by using the COS analysis method under state-of-the-art conditions. Because this method of analysis is still undergoing development, the limitations of this technique are not precisely defined. Furthermore, many questions still remain concerning plane-stress fracture generally, even for results obtained under LEFM conditions. Nevertheless, the present studies have been an encouraging first step in the understanding of the plane-stress fracture behavior of A572 Grade 50 steel, and similar medium-strength constructional steels, and of the applicability of plane-stress-fracture data (R-curve and K_c measurements) to structural components.

Acknowledgment

This study was supported by the American Iron and Steel Institute (AISI) and was conducted under AISI Project 168, entitled, "Toughness Criteria for Structural Steels." The tests of the 10 CT specimens under displacement-control conditions and the follow-up CVN tests on 7 of these specimens were conducted at the Armco Steel Corporation Research Center in Middletown, Ohio, under the direction of D. E. McCabe and R. H. Heyer. The author gratefully acknowledges this vital contribution, as well as the frequent discussions on R-curve technology with Messrs. McCabe and Heyer. Additional frequent discussions with the author's colleague, J. M. Barsom, are also hereby acknowledged. Thanks are also extended to J. F. Sovak for conducting the R-curve tests and making the subsequent calculations. Additional gratitude is also extended to Betty K. Stewart for helpful discussions concerning the application of statistical analysis concepts.

References

1. Fracture Toughness Evaluation by R-Curve Methods, (ASTM STP 527), ASTM, Philadelphia, 1973.

2. R. H. Heyer, "Crack Growth Resistance Curves (R-Curves)—Literature Review," ASTM STP 527, pp. 1-16.

3. R. H. Heyer and D. E. McCabe, "Plane-Stress Fracture Toughness Testing Using a Crack-Line-Loaded Specimen," Engineering Fracture Mechanics, Vol. 4, 1972, p. 393.

4. R. H. Heyer and D. E. McCabe, "Crack Growth Resistance in Plane-Stress Fracture Testing," Engineering Fracture Mechanics, Vol. 4, 1972, pp. 413-430.

5. "Proposed Recommended Standard for R-Curve Determination," presented (by D. E. McCabe) at the ASTM E-24 committee meetings held at Williamsburg, Virginia, March 6 to 8, 1973.

6. A. A. Wells, "Notched Bar Tests, Fracture Mechanics, and the Brittle Strengths of Welded Structure," British Welding Journal, vol. 12, No. 2, 1962.

7. A. A. Wells, "Crack Opening Displacements from Elastic-Plastic Analyses of Externally Notched Tension Bars," Engineering Fracture Mechanics, Vol. 1, No. 3, April, 1969, pp. 399-410.

8. G. R. Irwin, "Linear Fracture Mechanics, Fracture Transition, and Fracture Control," Engineering Fracture Mechanics, Vol. 1, No. 2, August 1968, pp. 241-257.

9. D. E. McCabe and R. H. Heyer, "R-Curve Determination Using a Crack-Line-Wedge-Loaded (CLWL) Specimen," ASTM STP 527, pp. 17-35.

10. J. M. Barsom, J. F. Sovak, and S. R. Novak, "AISI Project 168—Toughness Criteria for Structural Steels: Fracture Toughness of A572 Steels," U. S. Steel Research Laboratory Report 97.021-001(2), December 29, 1972.

11. C. G. Schilling, K. H. Klippstein, G. T. Blake, S. R. Novak, and J. M. Barsom, "AISI Project 168—Toughness Criteria for Structural Steels: Low-Temperature Tests of Simulated Bridge Members," U. S. Steel Research Laboratory Report 97.021-001(3), December 31, 1972.

12. American Society for Testing and Materials, "Proposed Method of Test for Plane-Strain Fracture Toughness of Metallic Materials," Part 31, ASTM Standards, 1971, pp. 919-935.

13. S. R. Novak, "Effect of Prior Uniform Plastic Strain on the K_{Iscc} of High-Strength Steels in Sea Water," Engineering Fracture Mechanics, Vol. 5, pp. 727-763, 1973.

14. J. M. Barsom, J. F. Sovak, and S. R. Novak, "AISI Project 168—Toughness Criteria for Structural Steels: Fracture Toughness of A36 Steel," U. S. Steel Research Laboratory Report 97.021-001(1), May 1, 1972.

15. W. F. Brown, Jr., and J. E. Srawley, editors, Plane-Strain Crack Toughness Testing of High Strength Metallic Materials, (ASTM STP 410), ASTM, Philadelphia, 1967, pp. 26-27.

16. D. E. McCabe, "Evaluation of the Compact Tension Specimen for Determining Plane-Strain Fracture Toughness of High Strength Materials," Journal of Materials, Vol. 7, No. 4, December 1972, pp. 449-454.

17. J. M. Barsom and S. T. Rolfe, "K_{Ic} Transition-Temperature Behavior of A517-F Steel," Engineering Fracture Mechanics, Vol. 2, 1971, pp. 341-357.

18. E. T. Wessel, "Linear Elastic Fracture Mechanics for Thick-Walled Welded Steel Pressure Vessels—Material Property Considerations," Practical Fracture Mechanics for Structural Steel, Risley: Chapman and Hall, Ltd., 1969, pp. H1-H44.

19. J. A. Begley and P. R. Toolin, "Fracture Toughness and Fatigue Crack Growth Rate Properties of a Ni-Cr-Mo-V Steel Sensitive to Temper Embrittlement," Westinghouse Research Laboratory Scientific Paper 71-1E7-BFSGT-P-1, presented at the Fourth National Symposium on Fracture Mechanics held at Carnegie-Mellon University, August 1970, and submitted for publication to International Journal of Fracture Mechanics.

20. J. M. Barsom, "AISI Project 168—Toughness Criteria for Structural Steels: Investigation of Toughness Criteria for Bridge Steels," U. S. Steel Research Laboratory Report 97.018-001(5), February 8, 1973.

21. J. D. Landes and J. A. Begley, "The Effect of Specimen Geometry on J_{Ic}," Fracture Toughness, Part II (ASTM STP 514), September 1972, pp. 24-40.

22. R. J. Bucci, P. C. Paris, J. D. Landes, and J. R. Rice, "J-Integral Estimation Procedures," Fracture Toughness, Part II (ASTM STP 514), pp. 40-70.

23. P. C. Paris and G. C. Sih, "Stress Analysis of Cracks," Fracture Toughness Testing and Its Applications (ASTM STP 381), April 1965, pp. 30-83.

24. H. Tada, P. C. Paris, and G. R. Irwin, editors, Stress Analysis of Cracks Handbook, Del Research Corporation, Hellertown, Pa., 1973.

Glossary of Symbols

CCT	=	Center-cracked tension specimen.
CLWL	=	Crack-line wedge-loaded specimen.
COS	=	Crack-opening stretch.
CT	=	Compact-tension specimen.
CVN	=	Charpy V-notch specimen.
EDM	=	Electrical-discharge-machine process.
LEFM	=	Linear-elastic fracture mechanics.
PTC	=	Partial-thickness-crack specimen.
RD	=	Rolling direction.
L-T	=	Orientation of full-thickness crack stressed parallel to RD and propagating perpendicular to RD.
R-curve	=	Plot of K_R vs Δa, where $\Delta a \equiv \Delta a_{phy}$.
a	=	Crack length; crack depth for PTC specimen.
a_{cr}	=	Critical crack length for the onset of a particular event.
a_{eff}	=	Effective crack length, including r_p.
a_n	=	Machined-notch crack length.
a_o	=	Initial crack length.
a_{phy}	=	Physical or actual crack length.
a_{act}	=	Actual or physical crack length.
Δa	=	Increment of crack extension.
Δa_c	=	Critical increment of stable crack extension at fracture instability, a property of the R-curve.
r_p	=	Plane-stress plastic-zone radius at the crack tip.
r_{Ip}	=	Plane-strain plastic-zone radius at the crack tip.
h	=	Hinge point, a distance measured from the load line, P.
B	=	Specimen thickness.
J-Integral	=	Path-independent integral of plastic strain-energy density surrounding the crack tip.
J_{Ic}	=	Critical J_I value at fracture under plane-strain conditions (analogous to G).
E	=	Modulus of elasticity.
G	=	Crack-extension force or strain-energy release rate.
G_R	=	Resistance to crack extension measured in terms of G.
H	=	One half of CT specimen height.
K	=	Stress-intensity factor.
K_c	=	Critical K value at fracture under plane-stress conditions.
K_I	=	Applied K value under opening-mode (Mode I) loading conditions.
K_{Ic}	=	Critical K_I value at fracture under plane-strain conditions.

K_{Icr} = A general critical K_I value corresponding to the onset of a specific event (K_c, K_{Ic}, K_{Id}, K_{Iscc}, etc.).

K_{Id} = Value of K_{Ic} measured under dynamic or impact loading conditions.

$K_{I,Gub}$ = Greatest-upper-bound K_I value for plane-strain conditions.

$K_{I,Lub}$ = Least-upper-bound K_I value for plane-strain conditions.

$K_{I,max}$ = Nominal K_I value at fracture calculated using initial crack length (a_o) and maximum load (P_{max}) on the basis of LEFM analysis.

K_Q = Questionable or invalid K_{Ic} value based on 5 percent secant-intercept method of analysis in fracture test record.

K_R = Resistance to crack extension measured in terms of K.

$K_{R,pl}$ = Plateau value of K_R from an R-curve.

ΔK_f = Stress-intensity range used in fatigue precracking.

P = Load or force.

P_{max} = Maximum load in a fracture test.

R = Stress ratio used in fatigue precracking.

T = Temperature.

V = Crack-opening displacement measured with a clip gage.

V_1 = Value of V measured at a distance 0.1576W from the load line, P, counter to the crack extension direction.

$V_{1\ abs}$ = Absolute value of V_1.

V_2 = Value of V measured at a distance 0.303W from the load line, P, in the same direction as crack extension.

$V_{2\ abs}$ = Absolute value of V_2.

$(V_1/V_2)_s$ = Slope of V_1 vs V_2 test record measured under elastic unloading conditions.

W = Specimen width.

β = Limit of plane-strain conditions at value of $\beta = 0.4$.

δ = Crack-opening stretch or crack-tip dislocation, used interchangeably with COS.

ε = Strain.

$\dot{\varepsilon}$ = Strain rate.

ε_{zz} = Through-thickness strain.

ε_{BS} = Back-surface strain measured on the free surface opposing the crack at a location that intersects with the crack plane.

ε_{ys} = Yield strain.

ρ = Root radius of a machined notch tip.

σ = Stress; also, standard deviation in a statistical sense.

σ_D = Design stress; alternatively, the gross, uniform tension stress applied to a CCT specimen remotely.

σ_{ys} = Yield stress.

σ_{zz} = Through-thickness stress (synonymous with "constraint").

Table I

Chemical Composition of A572 Steel Tested—Percent

Yield Strength, ksi	C	Mn	P	S	Si	Cu	Ni	Cr	Mo	V	Ti	Al*	Al**	N***	Cb	O
50	0.21	1.20	0.010	0.023	0.24	0.026	0.014	0.029	0.010	0.049	<0.005	0.021	0.023	0.006	<0.005	0.0031
62	0.22	1.21	0.014	0.022	0.25	0.021	0.014	0.020	0.005	0.070	<0.005	0.046	0.050	0.012	<0.01	ND

* Acid-soluble.

** Total.

*** Kjeldahl determination.

ND - Not determined.

Conversion Factor:

1 ksi = 6.895 MN/m^2

Table II

Mechanical Properties of A572 Steel Tested

Yield Strength, ksi	Orientation	Yield Strength (0.2% Offset), ksi	Tensile Strength, ksi	Elongation in 1 Inch, %		Reduction of Area, %		Charpy V-Notch Energy Absorption, ft-lb		
				At Maximum Load	At Fracture	At Maximum Load	At Fracture	+70 F	+40 F	0 F
50	Longitudinal	50	83	ND	30.0	ND	69.0	38	28	4
62	Longitudinal	62	92	14.0	27.0	15.1	65.1	26	11	7
50	Transverse	50	81	ND	26.0	ND	56.3	21	14	7
62	Transverse	63.5	94	13.4	23.4	14.0	50.3	16	10	7

Conversion Factors:

1 ksi = 6.895 MN/m^2
1 inch = 25.4 mm
1 ft-lb = 1.36 J

Table III

Overall R-Curve Study

σys, ksi	Specimen Thickness, Inches	No. of Spec	Spec Type*	Test Temperatures**
50	B = 1.5	3	2T	T = −40 F, +40 F + +72 F
"	"	3	4T***	" " "
"	"	4	4C***	" " "
"	"	4	7C	" " "
"	B = 0.5****	4	2T	" " "
"	"	4	4T	" " "
		22 Total		
62	B = 1.5	2	7C	T = −40 F + +72 F
		2 Total		

* 2T and 4T specimens tested under "load-control" conditions, 4C and 7C specimens tested under "displacement-control" conditions.

** At least one specimen for each group of 3 or 4 was tested at each of the (nominal) test temperatures cited.

*** The cited 4T and 4C specimens provided an "overlapping" condition for each of the two different test techniques.

**** All B = 0.5-inch specimens were taken from that portion of the plate closest to the center after the original 1.5-inch plate thickness was split.

Table IV

Summary of Test Conditions, Specimen Measurement Capacities, and Nominal Fracture Behaviors*

Item No.	Specimen No.**	Specimen Size and Type	B,*** inches	Test Temperature, F	σ_{ys},# ksi	$K_{I,lub}$,## ksi $\sqrt{inch}$	K_{MC},### ksi $\sqrt{inch}$	K_{BSY},+ ksi $\sqrt{inch}$	P_{max}, pounds	P_{frac}, pounds	$V_{1,max}$,++ inch	$V_{1,frac}$,+++ inches	$K_{I,max}$,++++ ksi $\sqrt{inch}$
A. Full-Thickness Specimens (B = 1-1/2 Inches) of ASTM A572 Grade 50 (σ_{ys} = 50 ksi)													
1	7-1	2T	1.5	-35	55.4	42.8	57.4	74.3	39,900	39,900	0.047	0.047	110.1
2	7-2	2T	1.5	+34	51.3	39.6	54.0	70.3	45,850	45,850	0.114	0.114	122.8
3	7-3	2T	1.5	+67	50.3	38.9	53.3	69.7	34,650	34,650	0.034	0.034	91.3
4	7-2⊛	4T	1.5	-42	55.6	43.0	89.4	121.3	88,000	88,000	0.075	0.075	143.0
5	A7-4	4C	1.5	-40	55.6	43.0	85.7	112.8	55,900[1]	55,900[1]	0.044	0.044	102.8
6	7-3⊛	4T	1.5	+38	51.2	39.6	83.8	114.8	114,500	114,500	0.247	0.247	180.2
7	A7-1	4C	1.5	+40	51.2	39.6	78.0	102.1	66,400[2]	66,400[2]	0.085	0.085	124.0
8	A7-3	4C	1.5	+40	51.2	39.6	78.3	104.5	77,400[2]	77,400[2]	0.126	0.126	140.1
9	7-1⊛	4T	1.5	+72	50.2	38.8	79.5	106.9	106,500	97,500	0.334	0.476	177.2
10	A7-2	4C	1.5	RT	50.2	38.8	77.0	101.2	92,900[2]	84,400[2]	0.155	0.273	170.5
11	A572-1	7C	1.5	-44	55.7	43.1	112.8	149.6	41,600[1]	41,600[1]	0.031	0.031	54.8
12	A7-3	7C	1.5	-40	55.6	43.0	112.2	147.8	73,600[1]	73,600[1]	0.058	0.058	102.0
13	A7-4	7C	1.5	+40	51.2	39.6	103.2	135.8	116,200[1]	116,200[1]	0.111	0.111	161.3
14	A572-2	7C	1.5	RT	50.2	38.8	102.3	135.2	159,300[2]	<86,900[2]	0.262	0.599	208.5
B. Full-Thickness Specimens (B = 1-1/2 Inches) of ASTM A572 Processed to σ_{ys} = 62 ksi													
15	A7-1	7C	1.5	-40	67.8	52.5	136.0	178.8	80,100[1]	80,100[1]	0.068	0.068	113.6
16	A7-2	7C	1.5	RT	62.2	48.2	126.4	167.8	134,100[2]	123,400[2]	0.200	0.326	184.8
C. Subthickness Specimens (B = 1/2 Inch) of ASTM Grade 50 (σ_{ys} = 50 ksi)													
17	7-3	2T	0.5	-32	55.3	24.7	57.4	74.4	15,200	15,150	0.158	0.202	124.5
18	7-2	2T	0.5	+32	51.3	22.9	53.9	70.2	16,200	16,150	0.192	0.222	129.8
19	7-1	2T	0.5	+32	51.3	22.9	54.0	70.3	15,750	15,400	0.198	0.258	125.8
20	7-4	2T	0.5	+66	50.3	22.5	52.3	67.8	15,300	13,700	0.193	0.329	125.3
21	7-4⊛	4T	0.5	-40	55.6	24.9	90.2	122.6	30,700	30,700	0.077	0.077	146.5
22	7-3⊛	4T	0.5	+39	51.2	22.9	82.3	111.8	37,800	37,700	0.251	0.251	132.6
23	7-2⊛	4T	0.5	+72	50.2	22.5	82.3	112.8	38,700	<10,200[3]	0.290	>>1.527	161.0
24	7-1⊛	4T	0.5	+72	50.2	22.5	81.6	111.2	37,700	3,300[4]	0.313	>1.748	179.3

(Continued)

Table IV (Continued)

* All specimens were of the compact-tension (CT) with (H/W) = 0.600; all 2T and 4T specimens were tested (by U. S. Steel Corporation) under load-control conditions, and all 4C and 7C specimens were tested (by Armco Steel Corporation) under displacement-control conditions.

** All specimen numbers with an "A" prefix (4C or 7C specimen types) were tested (by Armco Steel Corporation) under displacement-control. conditions.

*** Nominal specimen thickness -

\# σ_{ys} = **yield**-strength (0.2% offset) values interpolated at the test temperatures shown using actual measurements made (as a function of **temperature**) under "static" test conditions ($\dot{\epsilon} \cong 10^{-5}$ sec^{-1}).

\## $K_{I,lub}$ = plane-strain measurement capacity (least-upper-bound), given as: $K_{I,lub} = \sigma_{ys}\left(\frac{B}{2.50}\right)^{1/2}$.

\### K_{MC} = plane-stress measurement capacity (first conservative value - corresponding to $\sigma_N = \sigma_{ys}$ at the crack tip), given as:

$$K_{MC} = \sigma_{ys} \cdot W^{1/2}\left(\frac{f(X)\ (1-X)^2}{2(2+X)}\right) \text{ where } X = \left(\frac{a}{W}\right) \text{ and } f(X) = f\left(\frac{a}{W}\right) \text{ for the CT specimen.}$$

\+ K_{BSY} = plane-stress measurement capacity (second conservative value - corresponding to $\sigma_N = \sigma_{ys}$ at the back surface), given as:

$$K_{BSY} = -\sigma_{ys} \cdot W^{1/2}\left(\frac{f(X)\ (1-X)^2}{2(1+2X)}\right) \text{ where } X = \left(\frac{a}{W}\right) \text{ and } f(X) = f\left(\frac{a}{W}\right) \text{ for the CT specimen.}$$

++ $V_{1,max}$ = V_1 value at **maximum load** (@ $P = P_{max}$) in the P-V_1 record.

+++ $V_{1,frac}$ = V_1 value at the unstable fracture load (@ $P = P_{frac}$) in the P-V_1 test record.

Note: The V_1 values for each of the two previous footnotes were either measured directly (in the case of the <u>10</u> 4C and 7C specimens tested under deflection-control conditions) or interpolated values calculated assuming "rigid-body behavior" between the V_1 and V_2 (measured) clip-gage values (in the case of the <u>14</u> 2T and 4T specimens tested under load-control conditions).

++++ $K_{I,max}$ = nominal K_I value at maximum load ($P = P_{max}$), calculated on the basis of the original specimen dimensions without any corrections to the original (physical) crack length (a_o) for plasticity (r_p) or stable crack extension (Δa), given as:

$$K_I = \left[\frac{P \cdot f\left(\frac{a}{W}\right)}{B \cdot W^{1/2}}\right]$$

@ Specimen was tested using the "load-total unload" procedure, with various physical measurements of the specimen being made intermediately under no-load ($P = 0$) conditions (U. S. Steel procedure).

1) Load, P, was <u>calculated</u> using a_{eff} [based on $\left(\frac{V_{1abs}}{V_{2abs}}\right)$ ratio] and the <u>single-compliance calibration</u> relationship $\left[\left(\frac{EBV_1}{P}\right) \text{ vs } \left(\frac{a}{W}\right)\right]$.

2) Load, P, was <u>calculated indirectly</u> using a_{eff} and K_R in combination with the elastic stress-intensity relationship, $K_I = \left[\frac{P \cdot f\left(\frac{a}{W}\right)}{B \cdot W^{1/2}}\right]$.

The a_{eff} value was calculated using the <u>double-compliance calibration</u> relationship $\left[\left(\frac{V_1}{V_2}\right) \text{ vs } \left(\frac{a}{W}\right)\right]$ as $a_{eff} = a_{phy} + A\left(\frac{K_R}{\sigma_{ys}}\right)^2$, where A is a constant determined at $\epsilon_{BS} \cong \epsilon_{ys}$ - that is, when a_{eff} and a_{phy} are both known simultaneously with the use of the $\left(\frac{V_{1abs}}{V_{2abs}}\right)$ and $\left(\frac{V_1}{V_2}\right)_s$ ratios, respectively. This indirect (and approximate) method is necessary since a_{eff} <u>cannot</u> be determined directly using $\left(\frac{V_{1abs}}{V_{2abs}}\right)$ for $\epsilon_{BS} \gg \epsilon_{ys}$.

(Continued)

Table IV (Continued)

3) $P_{frac} \cong 6{,}200$ pounds, which occurred under increasing test-machine crosshead velocity and therefore at a crack-tip strain rate which is more rapid than that for "static" testing ($\dot{\varepsilon} >> 10^{-5}\ sec^{-1}$).

4) $P_{frac} = 3{,}300$ pounds, which occurred under increasing test-machine crosshead velocity and therefore at a crack-tip strain rate which is more rapid than that for "static" testing ($\dot{\varepsilon} >> 10^{-5}\ sec^{-1}$).

<u>Conversion Factors</u>:

1 inch = 25.4 mm

F = 9/5 C + 32

1 ksi = 6.895 MN/m^2

$1\ ksi\ \sqrt{inch} = 1.099\ MNm^{-3/2}$

1 pound = 4.448 N

Table V

Summary of R-Curve and K_c Test Results for ASTM A572 Steels*

Item No.	Specimen No.	Specimen Size and Type	B,** inches	Test Temperature, F	Specimens Tested Under Load Control*** Meas a_o, inches	DC a_o, inches	Mismatch Δa, inch	Specimens Tested Under Deflection-Control*** Meas a_o, inches	DC a_o, inches	Mismatch Δa, inch	$K_{R,max}$,# ksi $\sqrt{inch}$	Analysis Technique for Calc of $K_{R,max}$	Δa_{max},## inches	K_c,### ksi $\sqrt{inch}$
A. Full-Thickness Specimens (B = 1-1/2 Inches) of ASTM A572 Grade 50 (σ_{ys} = 50 ksi)														
1	7-1	2T	1.5	-35	1.784	1.720	-0.064	-	-	-	115.7	COS	0.044	116
2	7-2	2T	1.5	+34	1.739	1.728	-0.011	-	-	-	216.4	COS	0.034	216
3	7-3	2T	1.5	+67	1.714	1.603+	-0.111	-	-	-	87.4++	COS	0	>87++
4	7-2	4T	1.5	-42	2.988	2.797	-0.191	-	-	-	154.1	COS	0	154
5	A7-4	4C	1.5	-40	-	-	-	3.450	3.370	-0.080	101.9	LEFM	0	102
6	7-3	4T	1.5	+38	2.887	2.706	-0.181	-	-	-	313.7	COS	0.128	314
7	A7-1	4C	1.5	+40	-	-	-	3.530	3.440	-0.090	154.6	COS	0.020	155
8	A7-3	4C	1.5	+40	-	-	-	3.430	3.440	0.010	194.5	COS	0.125	195
9	7-1	4T	1.5	+72	3.077	2.894	-0.183	-	-	-	445.0	COS	0.477	445
10	A7-2	4C	1.5	RT	-	-	-	3.480	3.430	-0.050	318.3	COS	0.250	318
11	A572-1	7C	1.5	-44	-	-	-	5.750	5.750	0	56.8	LEFM	0	57
12	A7-3	7C	1.5	-40	-	-	-	5.830	5.730	-0.100	103.4	LEFM	0.020	103
13	A7-4	7C	1.5	+40	-	-	-	5.840	5.910	0.070	190.5	LEFM	0.120	191
14	A572-2	7C	1.5	RT	-	-	-	5.720	5.720	0	>477.3+++	COS	>0.868+++	>477+++
B. Full-Thickness Specimens (B = 1-1/2 Inches) of ASTM A572 Processed to σ_{ys} = 62 ksi														
15	A7-1	7C	1.5	-40	-	-	-	5.860	5.820	-0.040	121.4	LEFM	0.030	121
16	A7-2	7C	1.5	RT	-	-	-	5.720	5.740	0.020	364.5	COS	0.480	365
C. Subthickness Specimens (B = 1/2 Inch) of ASTM A572 Grade 50 (σ_{ys} = 50 ksi)														
17	7-3	2T	0.5	-32	1.775	1.895	0.120	-	-	-	315.5	COS	0#	316
18	7-2	2T	0.5	+32	1.738	1.775	0.037	-	-	-	273.0	COS	0.127	273
19	7-1	2T	0.5	+32	1.735	1.838	0.103	-	-	-	312.6	COS	0.105	313
20	7-4	2T	0.5	+66	1.773	1.612	-0.161	-	-	-	308.4	COS	0.399	308
21	7-4	4T	0.5	-40	2.945	2.786	-0.159	-	-	-	149.6	COS	0.023	150
22	7-3	4T	0.5	+39	2.976	2.771	-0.205	-	-	-	304.8	COS	0.216	305
23	7-2	4T	0.5	+72	2.871	2.726	-0.145	-	-	-	>502.8##	COS	>1.430##	>503##
24	7-1	4T	0.5	+72	2.933	2.773	-0.160	-	-	-	>379.6##	COS	>0.922##	>380##

(Continued)

Table V (Continued)

* All specimens were of the compact-tension (CT) type [with (H/W) = 0.600] and were of the same RW crack orientation (a through-thickness crack subjected to stresses parallel to the rolling direction, R, and propagating across the orthogonal plate width direction, W). In addition, all specimens were tested under "static" crack-tip strain-rate conditions ($\dot{\varepsilon} = 10^{-4}$ to 10^{-5} sec^{-1}); the 2T and 4T specimens were tested under load-control conditions, and all 4C and 7C specimens were tested under deflection-control conditions.

** Nominal specimen thickness - see Table III for precise specimen measurements (W, 2H, B and a).

*** Meas a_o = initial specimen fatigue-crack length obtained as the average of physical measurements made through the specimen thickness.

DC a_o = initial specimen fatigue-crack length obtained from the Double-Compliance (DC) procedure using the initial $\left(\frac{V_1}{V_2}\right)_s$ ratio.

Mismatch Δa = the numerical difference between the Meas a_o and DC a_o values.

\# $K_{R,max}$ = the highest K_R value obtained in the test prior to catastrophic crack extension and calculated using either the COS or LEFM analysis technique listed in the next column; in the COS technique, the $K_{R,max}$ value was calculated using the final $\left(\frac{V_1}{V_2}\right)_s$ ratio prior to fracture.

\#\# Δa_{max} = the amount of stable crack extension occurring in the test prior to catastrophic extension of the crack at the $K_{R,max}$ value; thus, $\Delta a_{max} = a_f - a_o$, where a_o and a_f are the initial and final a_{phy} values, respectively, determined using the initial and final $(V_1/V_2)_s$ ratios in combination with the double-compliance (DC) calibration relationship

$$\left[\left(\frac{V_1}{V_2}\right) vs \left(\frac{a}{W}\right)\right].$$

\#\#\# K_c = the K_c value observed at instability for the specified test conditions (including T, $\dot{\varepsilon}$, B, and a_o).

\+ Estimated value only - due to premature fracture prior to the scheduled first unloading step.

\+\+ Value based on an estimated $(V_1/V_2)_s$ ratio - an approximation necessary due to premature fracture prior to the scheduled first unloading step. Premature fracture resulted in part from a more rapid crack-tip strain rate ($\dot{\varepsilon}$) than normal for "static" loading; thus, the K_c value observed is much lower than would be expected normally on account of a slightly cooler temperature (67 F compared with 72 F) and a shorter crack length (2T specimen with a_o = 1.714 inches).

\+\+\+ The $K_{R,max}$, Δa_{max}, and K_c values cited are minimum values since they correspond to the point at which the allowable deflection capability (physical limit) was exceeded (without specimen failure) in the deflection-control testing machine.

\# For an unknown reason no crack extension ($\Delta a_{phy} = 0$) was indicated at fracture by the V_1 vs V_2 test record, even though a stable extension of Δa_{phy} = 0.125 inch actually occurred on the fracture surface (see Figure 16); consequently, an initial negative error of 7.5 percent in K_R at low load levels due to a Mismatch Δa = +0.120 inch was fully cancelled at $K_R = K_{R,max}$ by an equivalent positive error of 7.5 percent in K_R arising from the actual crack extension, Δa_{phy} = 0.125 inch.

\#\# The $K_{R,max}$, Δa_{max}, and K_c values cited are minimum values of behavior since they correspond to the highest values measured prior to the onset of erratic clip-gage behavior (V_1 and V_2) and occurred well before complete (catastrophic) specimen fracture. The erratic clip-gage behavior resulted, specifically, from a combination of circumstances including 1) exceeding the available clip-gage linearity range, 2) the occurrence of out-of-plane specimen buckling, and 3) concomitant misalignment of the clip-gage holders attached to the specimen. The cited Δa_{max} values (1.430 and 0.920 inches for specimens 7-2 and 7-1, respectively) can be seen to be only a small fraction of the total stable crack extension that took place on the fracture surfaces of each specimen prior to catastrophic crack extension, Δa_{max} = 3.471 and 3.954 inches for specimens 7-2 and 7-1, respectively (Figure 17).

Conversion Factors:

1 inch = 25.4 mm   1 ksi $\sqrt{inch}$ = 1.099 $MNm^{-3/2}$

F = 9/5 C + 32   1 ksi = 6.895 MN/m^2

Table VI

Analysis of K_C Results for Duplicate Specimen Tests

Item No.	No. of Specimens Tested	Specimen Size and Type	B, inches	Test Temperature, F	K_C, ksi $\sqrt{\text{inch}}$	Average K_C and Range, ksi $\sqrt{\text{inch}}$	Range of K_C Results,* percent
7&8	2	4C	1.50	+40	155 195	175±20	±11.4
11&12	2	7C	1.50	-40	57 103	80±23	±28.8
18&19	2	2T	0.50	+40	273 313	293±20	±6.8
23&24	2	4T	0.50	+72	>503 >380	>442±62	±14.0

* Range expressed of percent relative to the average K_c value cited in the previous column.

Conversion Factors:

1 inch = 25.4 mm

F = 9/5 C + 32

1 ksi $\sqrt{\text{inch}}$ = 1.099 $MNm^{-3/2}$

Table VII

Analysis of K_c Results for Different Test Procedures

Item No.	Specimen Size and Type*	Nominal Test Temperature, F	K_c, ksi $\sqrt{\text{inch}}$	Extent to Which K_c for 4T Exceeds That for 4C**
4	4T	-40	154	+51.0%
5	4C	-40	102	-
6	4T	+40	314	+79.5%
7	4C	+40	155	-
8	4C	+40	195	-
9	4T	+72	445	+40.0%
10	4C	+72	318	-

* 4T specimens tested by load-control test method.
4C specimens tested by deflection-control test method.

** Expressed as a percentage of the listed (or average) K_c value for the corresponding 4C specimen.

Conversion Factors:

$$F = 9/5\ C + 32$$
$$1\ \text{ksi}\ \sqrt{\text{inch}} = 1.099\ \text{MNm}^{-3/2}$$

Table VIII

Comparisons of Studies Conducted to Evaluate K_c Behavior Measured Using the Load-Control and Displacement-Control Test Techniques

	Earlier Studies by Heyer & McCabe*		Present Study**
Materials	High-Strength Aluminum & Titanium Alloys	vs	Low-Strength Steel
Material thickness, inches	$B \leq 0.066$	vs	$B = 1.50$
K_c Repeatability	Excellent (±5%)	vs	Fair (±15 to ±30%)
Strain-rate Sensitivity (on K_c)	NIL	vs	High
Method of Analysis @ K_c	LEFM	vs	COS

* Complete Equivalense of K_c behavior demonstrated in tests conducted with load-control and displacement-control testing techniques.

** K_c for load-control = 40% to 80% higher than K_c for displacement-control.

Table IX

Effects of Thickness (B = 1.5 inch vs B = 0.5 inch) on K_c Behavior from Load-Control Tests on 50-ksi Yield-Strength A572 Grade 50 Steel

Item No.	Specimen Size	Nominal Test Temperature, F	K_c for B = 1.50 inch Specimen, ksi $\sqrt{\text{inch}}$	K_c for B = 0.50 inch Specimen, ksi $\sqrt{\text{inch}}$
		A. 2T Specimen Size		
1	2T	-40	116	-
17	2T	-40	-	316
2	2T	+40	216	-
18	2T	+40	-	273
19	2T	+40	-	313
3	2T	+72	>87+	-
20	2T	+72	-	308
		B. 4T Specimen Size		
4	4T	-40	154	-
21	4T	-40	-	150
6	4T	+40	314	-
22	4T	+40	-	305
9	4T	+72	445	-
23	4T	+72	-	>503+
24	4T	+72	-	>380+

+ See appropriate footnote for detailed behavior in Table V.

Conversion Factors

1 inch = 25.4 mm.

F = 9/5C + 32.

1 ksi $\sqrt{\text{inch}}$ = 1.099 $MNm^{-3/2}$.

Table X

Summary of CVN Test Results From Selected CT Specimens of A572 Steel

Item No.	Specimen No.	Specimen Size and Type	B, inches	Test Temperature, F	K_c, ksi $\sqrt{\text{inch}}$	CVN Energy Absorption, ft-lb											
						+72 F				+40 F			0 F			-40 F	
3	7-3	2T	1.50	+67	>87	45.0	45.0	37.0	53.0	27.0	21.0	26.0	9.0	15.0	9.0	-	-
5	A7-4	4C	1.50	-40	102	49.5	38.5	56.0	44.5	49.0	-	35.0	-	-	-	12.0	17.0
7	A7-1	4C	1.50	+40	155	45.0	38.0	53.5	52.0	32.0	-	30.5	-	-	-	5.0	9.0
8	A7-3	4C	1.50	+40	195	50.0	41.0	47.0	38.0	42.0	-	29.0	-	-	-	2.5	7.0
9	7-1	4T	1.50	+72	445	41.0	41.0	56.0	-	26.0	30.0	26.0	24.0	-	23.0	-	-
10	A7-2	4C	1.50	RT	318	42.0	51.0	47.0	60.5	32.0	-	38.5	-	-	-	3.5	5.5
11	A572-1	7C	1.50	-44	57	47.0	47.5	74.0	54.0	40.0	-	39.5	-	-	-	3.0	6.0
12	A7-3	7C	1.50	-40	103	51.5	43.5	54.0	42.0	14.5	-	20.5	-	-	6.0	-	5.5
13	A7-4	7C	1.50	+40	191	43.0	45.5	30.0	41.0	25.0	-	32.0	-	-	-	3.5	2.5
17	7-3*	2T	0.50	-32	316	60.0	47.0	-	-	33.0	-	32.0	25.0	-	35.0	16.0*	18.0*
21	7-4#	4T	0.50	-40	150	60.0	52.0	-	-	42.0	-	33.0	29.0	-	28.0	10.0#	18.0#
						Corresponding CVN Lateral Expansion (LE), mils											
3	7-3	2T	1.50	+67	>87	46.0	44.0	37.0	52.0	29.0	24.0	28.0	12.0	16.0	12.0	-	-
5	A7-4	4C	1.50	-40	102	38.0	31.5	42.0	37.5	38.5	-	27.0	-	-	-	6.5	10.0
7	A7-1	4C	1.50	+40	155	39.5	31.0	42.0	38.5	23.5	-	25.5	-	-	-	0.5	3.5
8	A7-3	4C	1.50	+40	195	37.0	33.5	38.0	34.5	31.5	-	21.0	-	-	-	0	4.0
9	7-1	4T	1.50	+72	445	41.0	38.0	47.0	-	24.0	27.0	27.0	21.0	-	21.0	-	-
10	A7-2	4C	1.50	RT	318	35.0	44.0	38.0	48.0	24.5	-	29.0	-	-	-	2.0	0.5
11	A572-1	7C	1.50	-44	57	39.0	40.5	58.0	41.0	33.0	-	29.0	-	-	-	0	1.0
12	A7-3	7C	1.50	-40	103	41.0	36.0	41.5	35.0	13.0	-	15.0	-	-	-	1.0	1.5
13	A7-4	7C	1.50	+40	191	33.0	34.0	29.0	39.5	20.0	-	26.0	-	-	-	0	1.0
17	7-3*	2T	0.50	-32	316	51.0	40.0	-	-	31.0	-	32.0	24.0	-	32.0	14.0*	15.0*
21	7-4#	4T	0.50	-40	150	50.0	45.0	-	-	39.0	-	33.0	25.0	-	24.0	10.0#	15.0#

Note: * Additional results at -80 F were CVN energy = 6.0 and 4.0 ft-lb with corresponding LE = 3.0 and 2.0 mils.
Additional result at -80 F was CVN energy = 7.0 ft-lb and LE = 3.0 mils.

Conversion Factors:

1 inch = 25.4 mm
F = 9/5 C + 32
1 ksi $\sqrt{\text{inch}}$ = 1.099 $MNm^{-3/2}$
1 ft-lb = 1.36 J
1 mil = 0.0254 mm

Table XI

Summary of Static K_{Ic} Tests* on A572 Grade 50 (σ_{ys}=50 ksi) Steel

Item No.	Spec No.	Test Temp, F	σ_{ys}, ksi	Specimen Measurement Capacities: $K_{I,Lub}$,** ksi $\sqrt{inch}$	$K_{I,Gub}$*** ksi $\sqrt{inch}$	K_Q, ksi $\sqrt{inch}$	$\left(\frac{K_Q}{K_{I,Gub}}\right)$	$K_{I,max}$,+ ksi $\sqrt{inch}$	K_{Ic}, ksi $\sqrt{inch}$	Comments
1	7-1	-320	138	105	166	32.3	0.19	32.3	32.3	Valid
2	7-11	-320	138	106	168	25.7	0.16	26.2	25.7	Valid
3	7-8	-240	101	77	122	31.2	0.26	31.2	31.2	Valid
4	7-3	-220	94	72	114	36.2	0.32	36.2	36.2	Valid
5	7-13	-200	87	66	104	28.9	0.28	28.9	28.9	Valid
6	7-10	-180	81	62	98	38.3	0.39	38.3	38.3	Valid
7	7-4	-165	77	59	93	63.8	0.69	63.8	63.8	Essentially valid
8	7-8	-156	75	57	90	58.5	0.65	58.5	58.5	Essentially valid
9	7-9	-149	74	56	88	44.8	0.51	44.8	44.8	Valid
-	-	-	-	-	-	-	-	-	-	-
10	7-12	-120	67	51.5	81.5	76.5++	0.94	105.1	>51.5	Invalid
11	7-5	-104	64	49.0	77.5	74.2++	0.96	74.2	>49.0	Invalid
12	7-7	-55	57	43.2	68.3	73.6++	1.08	99.1	>43.2	Invalid
13	7-6	+7	52	39.9	63.1	71.9++	1.14	117.0	>39.9	Invalid
14	7-2	+75	50	38.0	60.1	63.4++	1.06	113.3	>38.0	Invalid

* 3-Point bend specimens: span = 24.0 inches [S/W = 4.0/1]; nominal specimen dimensions:

W = 6.00 inches
B = 1.47 inches
a = 2.90 inches

** Least-upper-bound measurement capacity, given as $K_{I,Lub} = \sigma_{ys}\left(\frac{B}{2.50}\right)^{1/2}$.

(Continued)

Table XI (Continued)

*** Greatest-upper-bound measurement capacity, given as $K_{I,Gub} = \sigma_{ys} \left(\frac{B}{1.00}\right)^{1/2}$.

+ Nominal K_I value at maximum load ($P = P_{max}$) calculated on the basis of LEFM and the original specimen dimensions, without any plasticity corrections to the original crack length, a.

++ K_Q value reflects <u>severe K_I-suppression effects</u> due to grossly inadequate specimen dimensions.

<u>Conversion Factors</u>:

$C = 5/9(F - 32)$
$1\ \text{ksi} = 6.895\ \text{MN/m}^2 = 6.895\ \text{N/mm}^2$
$1\ \text{ksi}\ \sqrt{\text{inch}} = 1.099\ \text{MNm}^{3/2}$
$1\ \text{inch} = 25.4\ \text{mm}$

Table XII

Fracture Behavior of A572 Grade 50 Steel (σys = 50 ksi)

	Invalid K_{Ic} Test Results		Estimated K_{Ic} Values, ksi $\sqrt{inch}$	
Test Temp	K_Q, ksi $\sqrt{inch}$	$\left(\frac{K_Q}{K_{I,Gub}}\right)$	From K_I-Suppression Effect*	From J-Integral**
-120 F	76.5	0.94	148^{-}	100-130
-104 F	74.2	0.96	148^{-}	-
-55 F	73.6	1.08	148^{+}	-
+7 F	71.9	1.14	148^{+}	-
+75 F	63.4	1.06	148^{+}	160-200

* $K_{Ic} \cong 2.0\ K_Q$ @ $\left(\frac{K_Q}{K_{I,Gub}}\right) = 1.00$ where $K_{I,Gub} = \sigma ys\left(\frac{B}{1.0}\right)^{1/2}$

$\therefore K_{Ic} \cong 2 \times 74 = 148$ ksi $\sqrt{inch}$ @ T = -80 F

** "One-shot" J_{Ic} equation.

Table XIII

Summary of Minimum Plane-Stress Fracture Toughness for Two Thicknesses of A572 Grade 50 Steel Under Static Loading Condiitons ($\dot{\varepsilon} \cong 10^{-5}$ sec^{-1})

Temperature, F	Minimum K_c, ksi $\sqrt{inch}$	σ_{ys}, ksi	Minimum a_{cr} for Infinite CCT Spec* @ $\sigma_D = 3/4\ \sigma_{ys}$, inches
A. For B = 1-1/2-Inch-Thick Plate and σ_{ys} = 50 ksi			
-40	57**	56	0.58 (180)**
+40	155	51	5.22
+72	318	50	22.9
B. For B = 1/2-Inch-Thick Plate and σ_{ys} = 50 ksi			
-40	150	56	4.06
+40	273	51	16.2
+72	>380	50	>32.7
C. For B = 1-1/2-Inch-Thick Plate and σ_{ys} = 62 ksi			
-40	121	68	1.80
+72	365	62	19.6

* For an infinite center-cracked tension (CCT) specimen:

$$K = \sigma\sqrt{\pi a} \tag{1}$$

Rearranging (1): $$\therefore a_{cr} = \frac{1}{\pi}\left(\frac{K_c}{\sigma_D}\right)^2 \tag{2}$$

and for

$$\sigma_D = 3/4\ \sigma_{ys}$$

we get

$$a_{cr} = \frac{16}{9\cdot\pi}\left(\frac{K_c}{\sigma_{ys}}\right)^2 = 0.566\left(\frac{K_c}{\sigma_{ys}}\right)^2 \tag{3}$$

** If the minimum representative fracture toughness is taken to be K_c = 100 ksi $\sqrt{inch}$; The corresponding value of critical flaw size would be a_{cr} = 1.80 inches.

Conversion Factors:

F = 9/5 C + 32

1 ksi $\sqrt{inch}$ = 1.099 $MNm^{-3/2}$

1 ksi = 6.895 N/mm^2 = 6.895 MN/m^2

1 inch = 25.4 mm

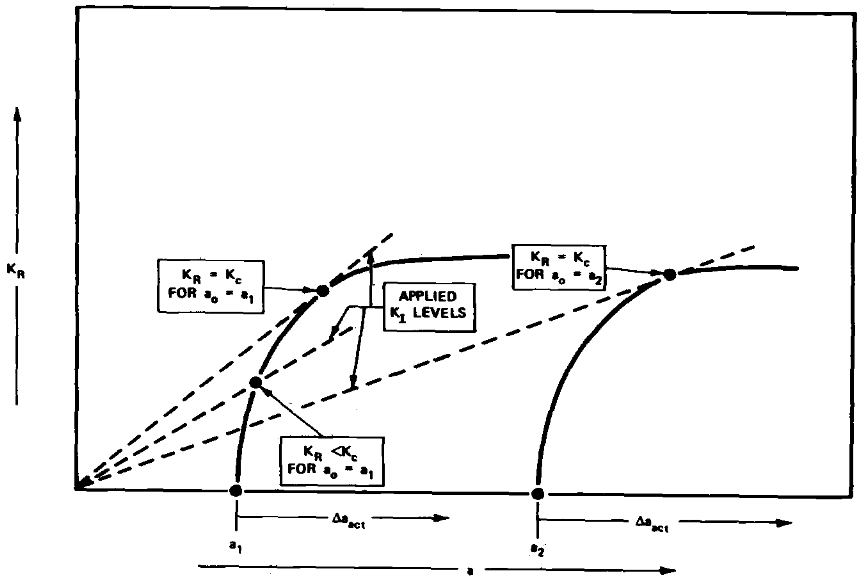

FIG. 1—*Basic principle of R-curves for use in determining K_c under different conditions of initial crack length, a_o.*

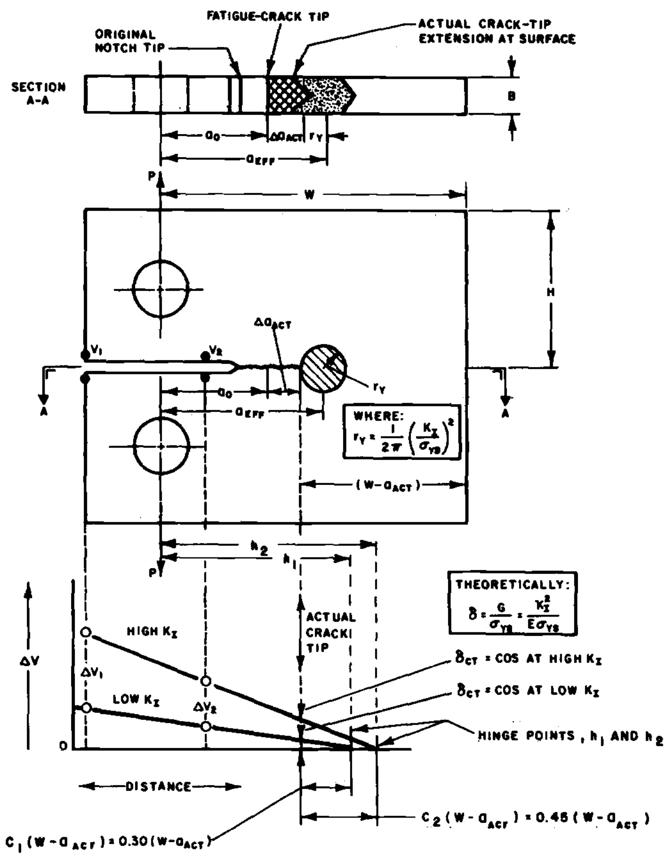

FIG. 2—*Schematic of procedure for measuring δ_{ct} or cos at the actual crack tip (σ_{act}) relative to applied load level (K_I) under plane-stress conditions.*

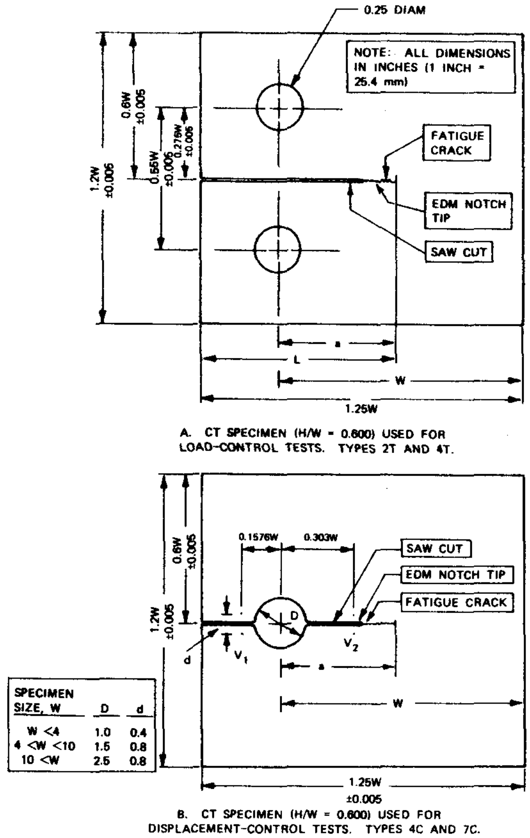

FIG. 3—*CT specimens used for load-control and displacement-control tests.*

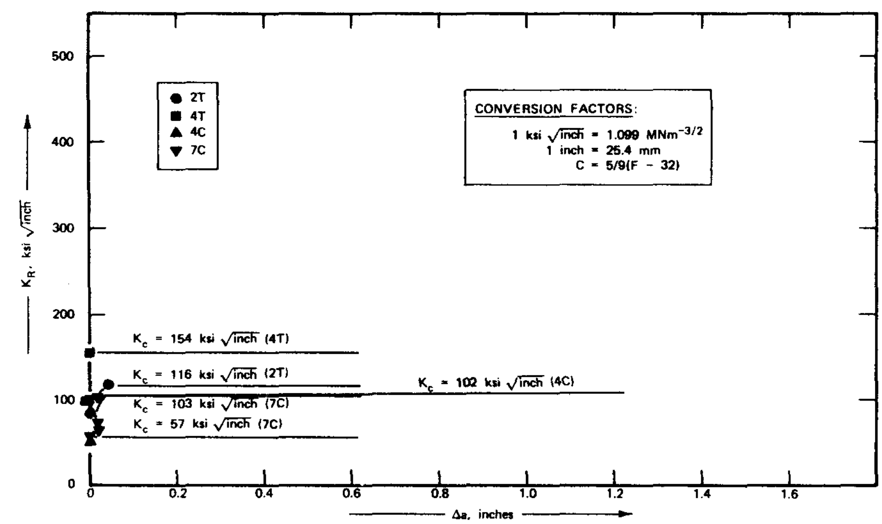

FIG. 4—*R-curve and K_c results of full-thickness (B = 1.5 in.) specimens of A572 Grade 50 steel tested at −40°F.*

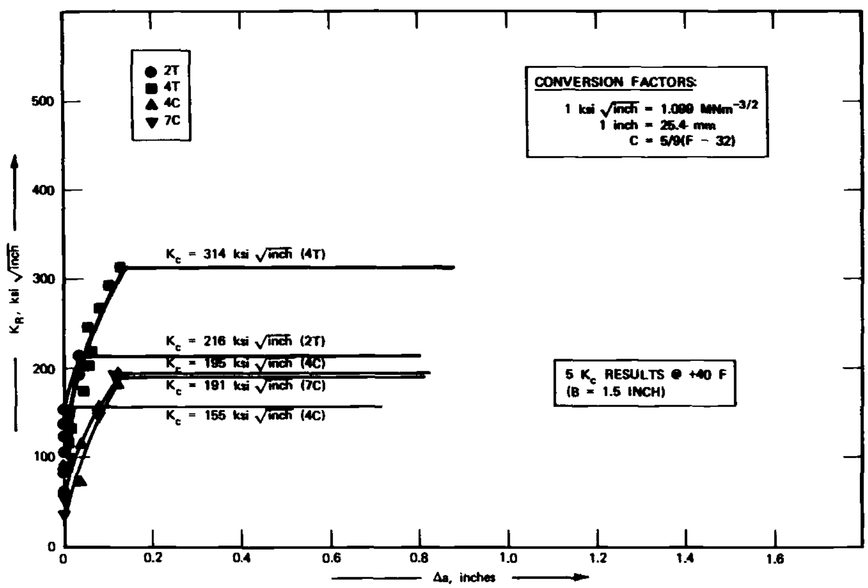

FIG. 5—*R-curve and K_c results for full-thickness ($B = 1.5$ in.) specimens of A572 grade 50 steel tested at +40°F.*

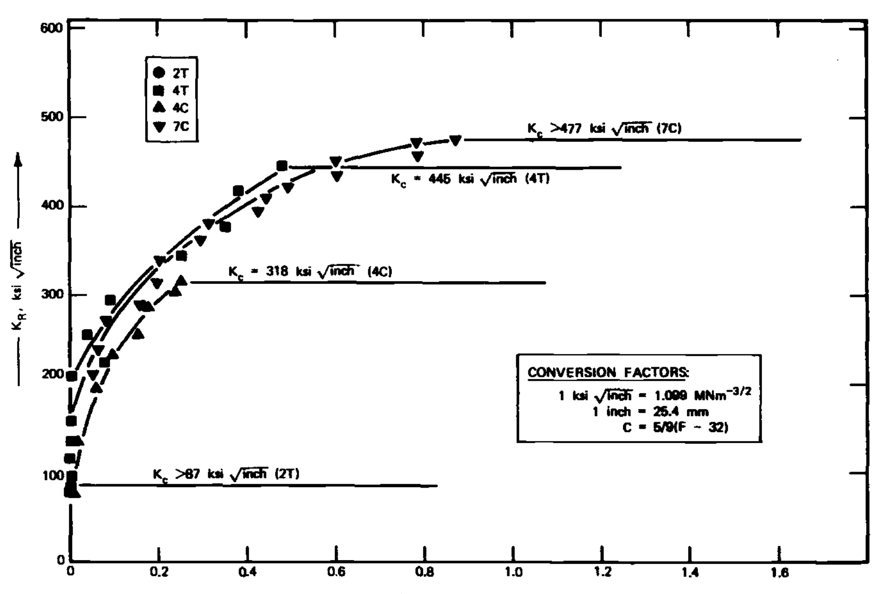

FIG. 6—*R-curve and K_c results for full-thickness ($B = 1.5$ in.) specimens of A572 grade 50 steel tested at +72°F.*

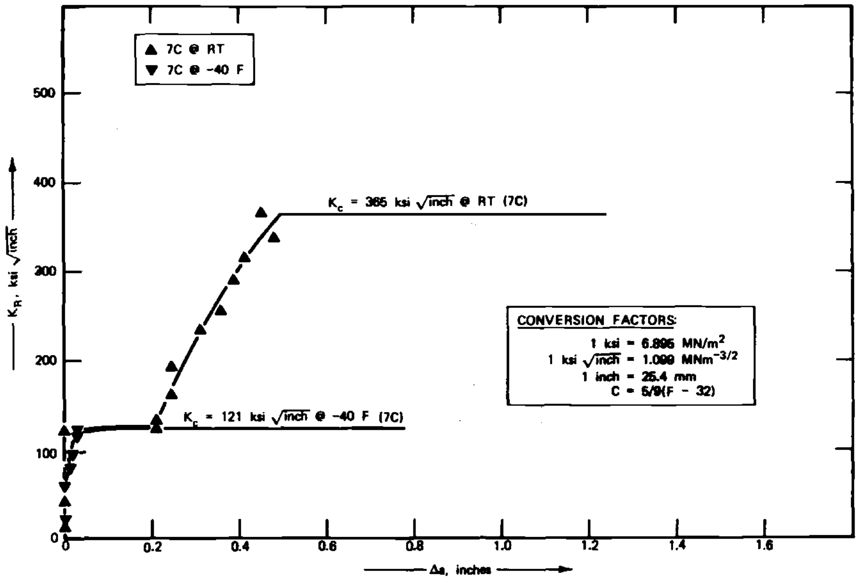

FIG. 7—*R-curve and K_c results for full-thickness (B = 1.5 in.) specimens of A572 steel processed to 62-ksi strength level at two different temperatures.*

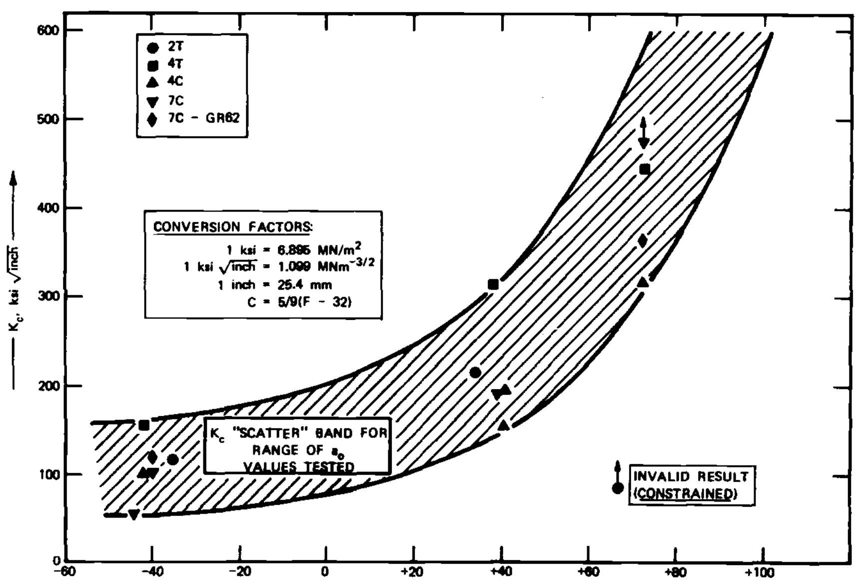

FIG. 8—*Summary of K_c results for full-thickness (B = 1.5 in.) specimens of A572 grade 50 steel and A572 steel processed to 62-ksi strength level.*

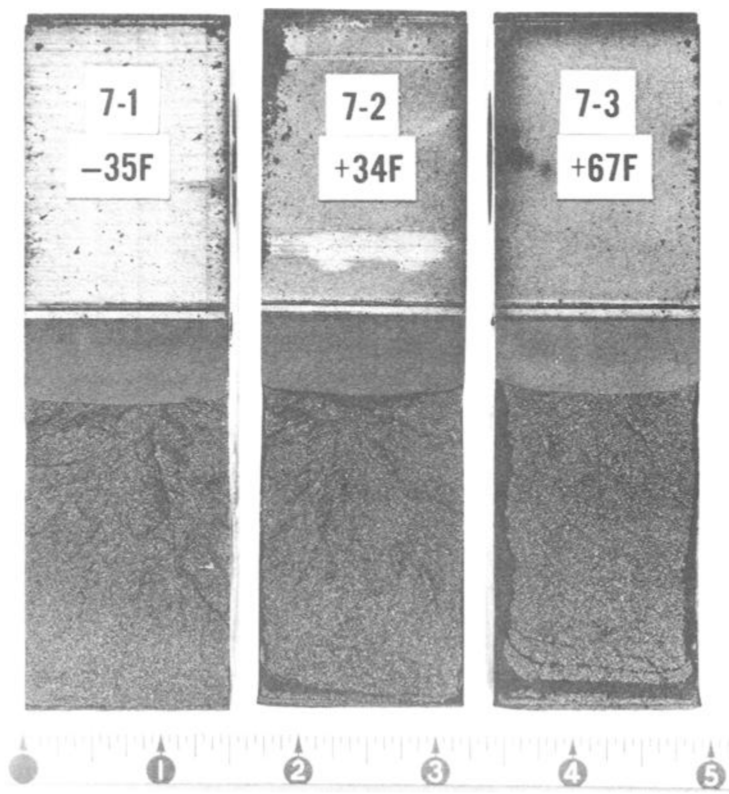

FIG. 9—*Fracture surfaces of full-thickness (B = 1.5 in.) 2T CT specimens of A572 grade 50 steel tested under load-control conditions using an essentially monotonic loading sequence (Armco procedure).*

FIG. 10—*Fracture surfaces of full-thickness (B = 1.5 in.) 4T CT specimens of A572 Grade 50 steel tested under load-control conditions using a total unload/reload loading sequence (U. S. Steel procedure).*

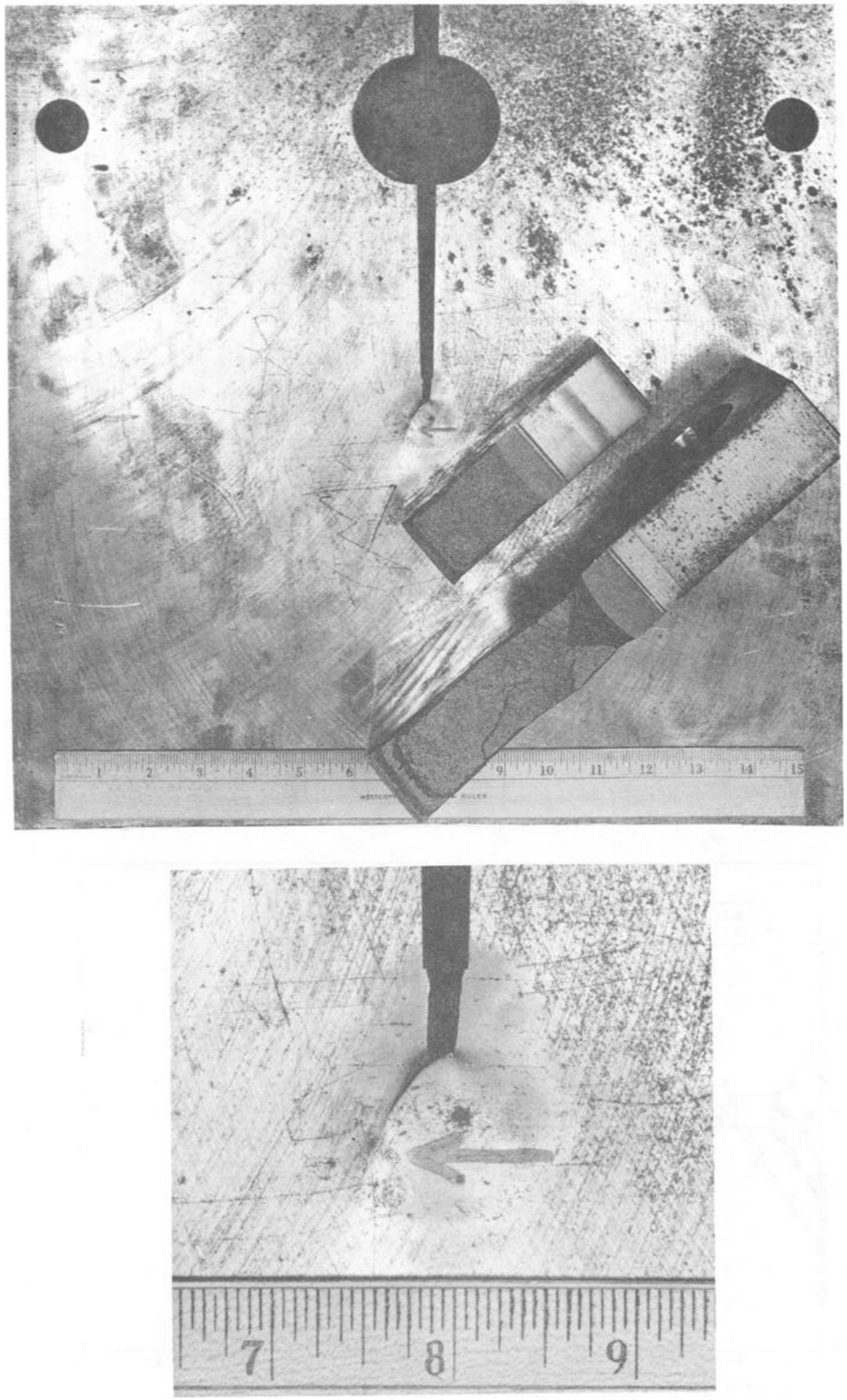

FIG. 11—*R-curve specimens of A572 Grade 50 steel tested at ambient temperature (~ 72°F). The 2T and 4T specimens were tested to fracture under load-control conditions, and the 7C specimen was tested to the limit of available capacity under displacement-control conditions. Note:* $\Delta a = a_f - a_o \cong 0.50$ *in. on the specimen surface for the 7C specimen at the end of the test.*

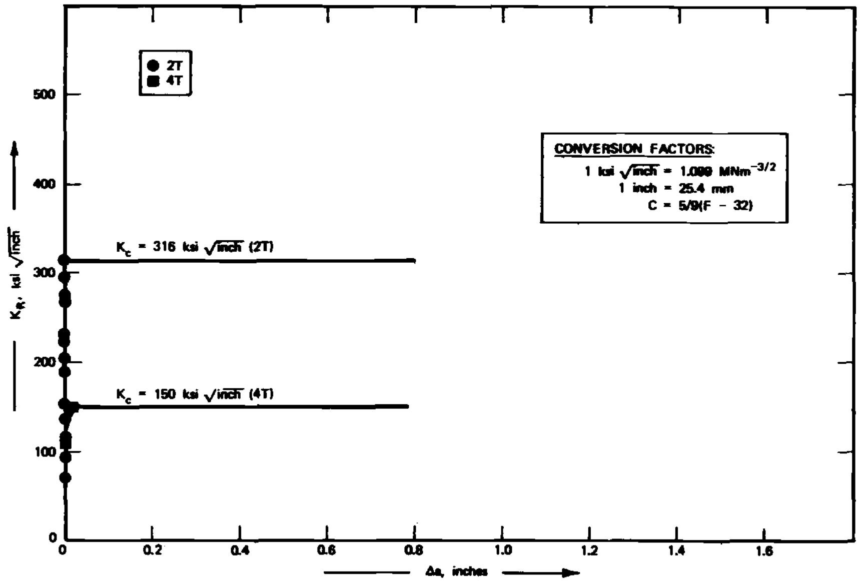

FIG. 12—*R-curve and K_c results for subthickness (B = 0.5 in.) specimens of A572 Grade 50 steel tested at −40°F.*

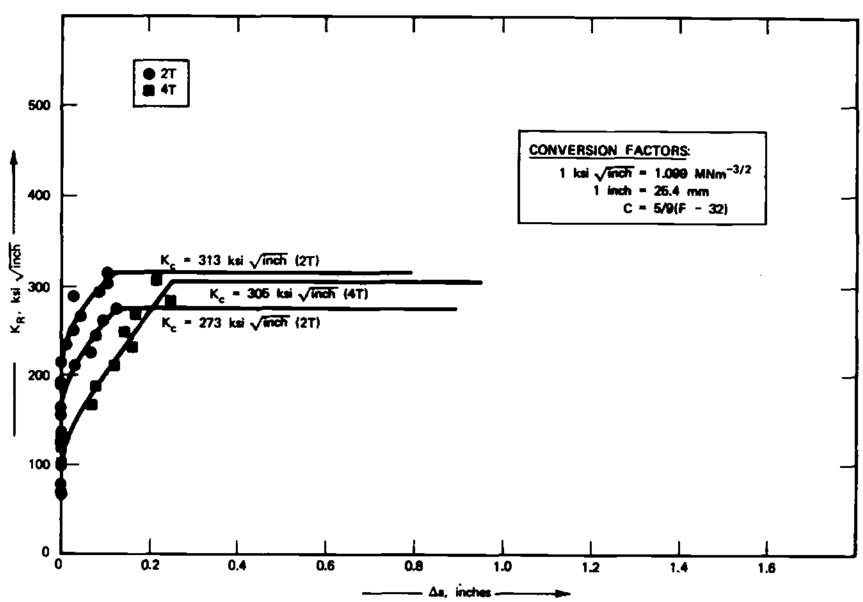

FIG. 13—*R-curve and K_c results for subthickness (B = 0.5 in.) specimens of A572 Grade 50 steel tested at +40°F.*

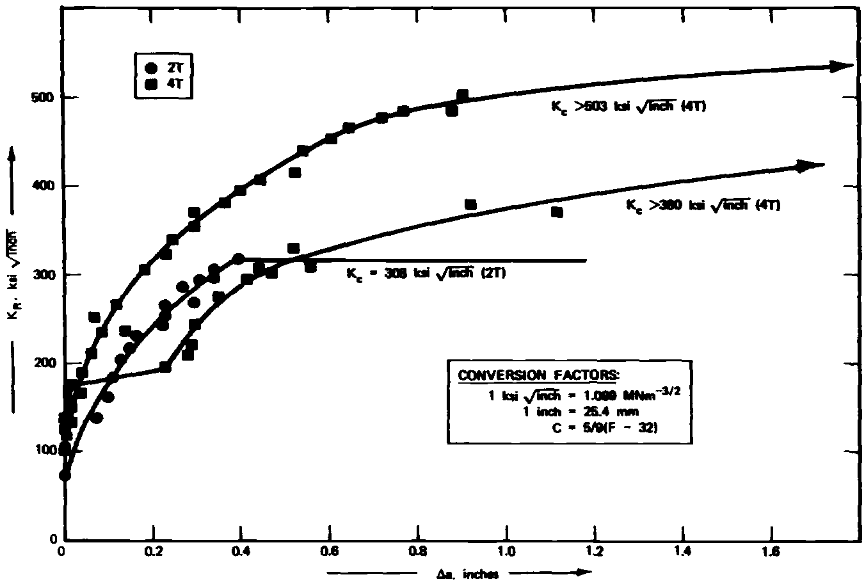

FIG. 14—*R-curve and K_c results for subthickness (B = 0.5 in.) specimens of A572 Grade 50 steel tested at +72°F.*

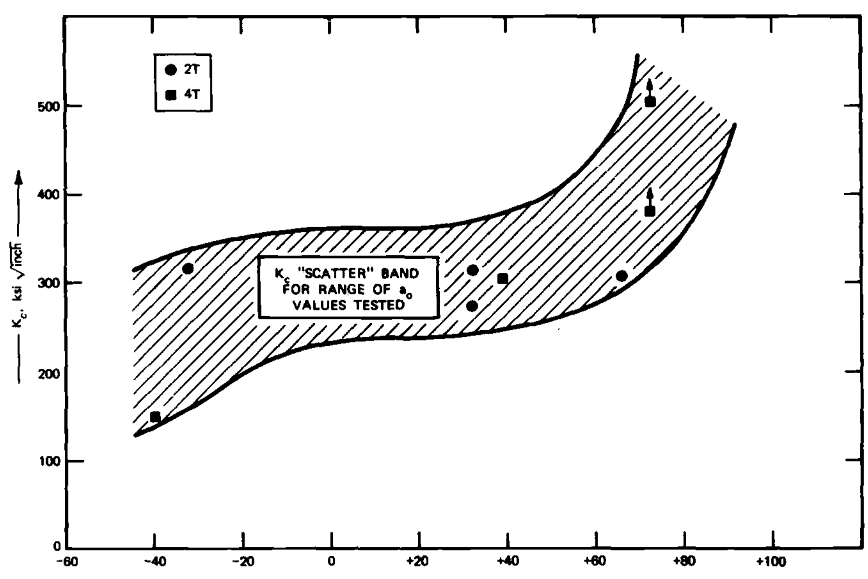

FIG. 15—*Summary of K_c results for subthickness (B = 0.5 in.) specimens of A572 Grade 50 steel.*

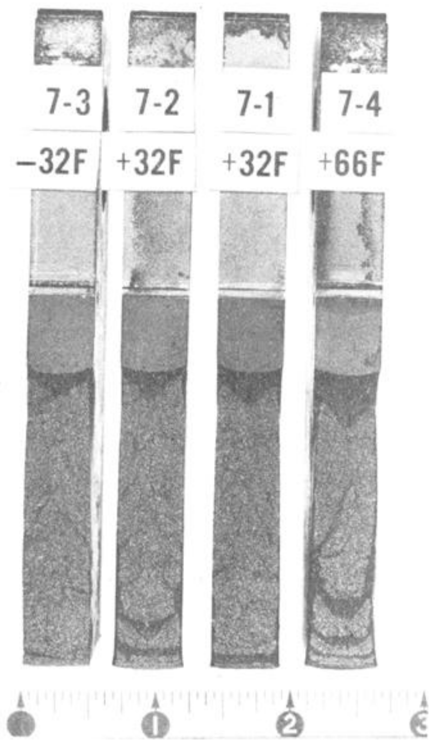

FIG. 16—*Fracture surfaces of subthickness (B = 0.5 in.) 2T CT specimens of A572 Grade 50 steel tested under load-control conditions using an essentially monotonic loading sequence (Armco procedure).*

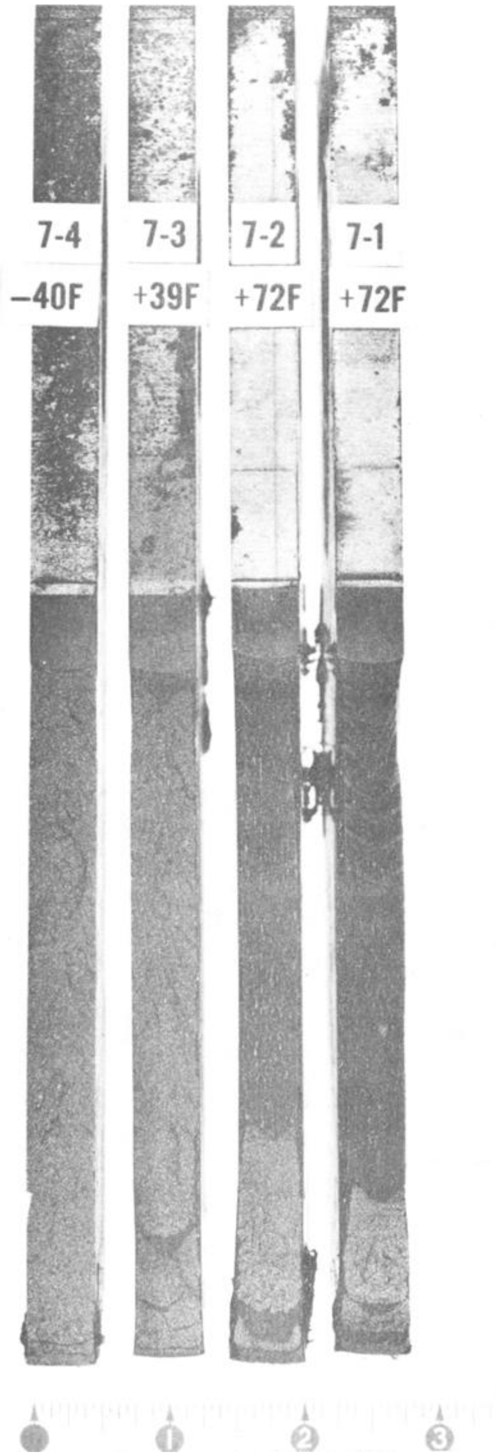

FIG. 17—*Fracture surfaces of subthickness (B = 0.5 in.) 4T CT specimens of A572 Grade steel tested under load-control conditions using a total unload/reload loading sequence (U. S. Steel procedure).*

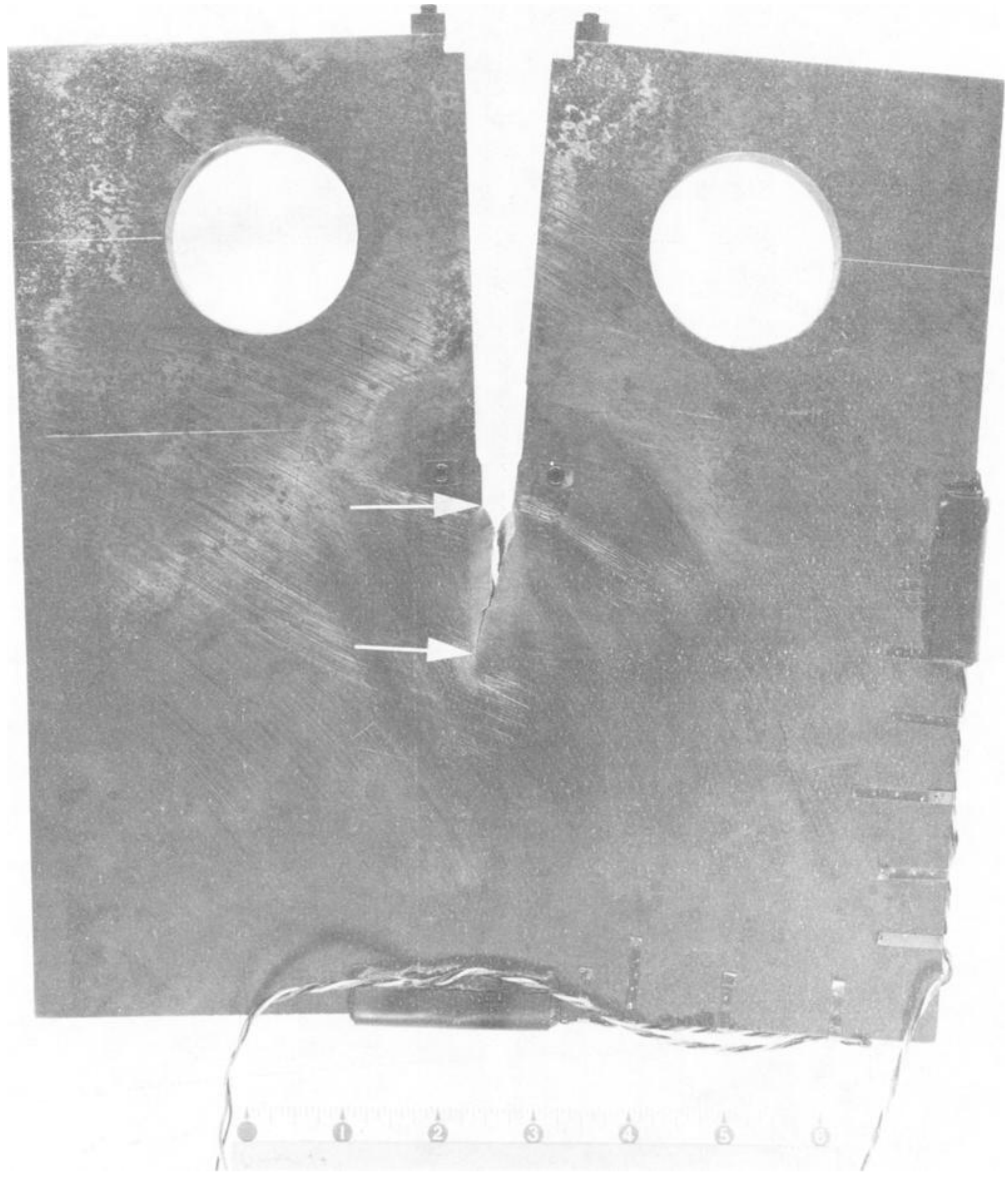

FIG. 18—*Subthickness ($B = 0.5$ in.) 4T CT specimen 7-2 tested at +72°F. Photograph was taken after unload 33 and just prior to complete fracture (intentional). Note the extent of stable crack extension visible on the specimen surface ($\Delta a = a_f - a_o \cong 1.60$ in.).*

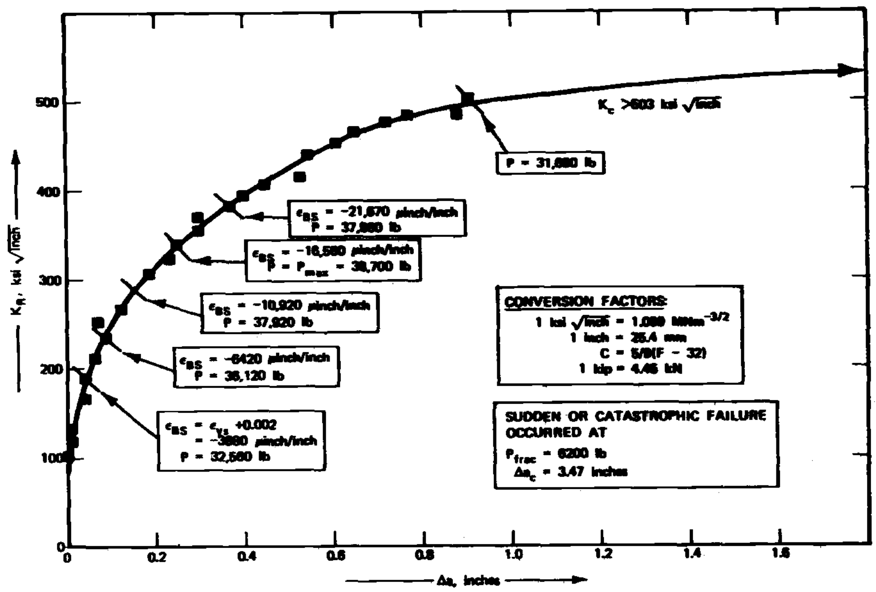

FIG. 19—*Superposition of ϵ_{BS} and P in the development for the 4T subthickness (B = 0.5 in.) specimen of A572 Grade 50 steel tested at +72°F.*

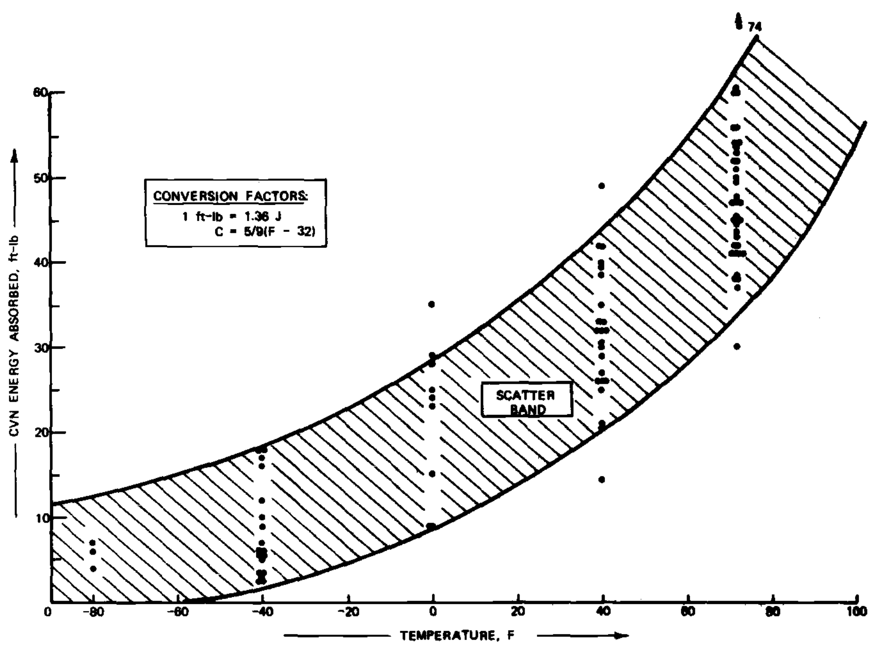

FIG. 20—*Combined CVN energy-absorption behavior of A572 Grade 50 steel as determined from the broken halves of 11 CT specimens used to establish R-curve behavior.*

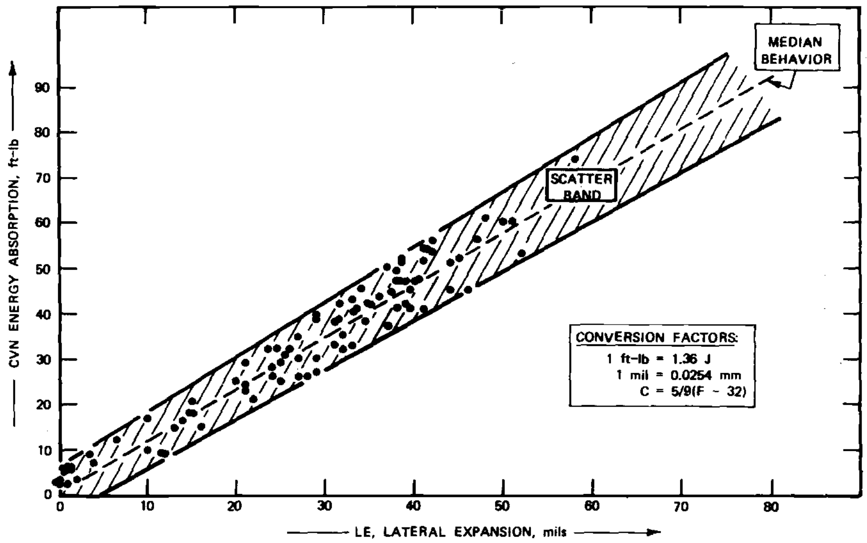

FIG. 21—*Correlation between CVN energy absorption and lateral expansion (LE) for A572 Grade 50 steel at all temperatures (−80 to +72°F) as determined from the broken halves of 11 CT specimens used to establish R-curve behavior.*

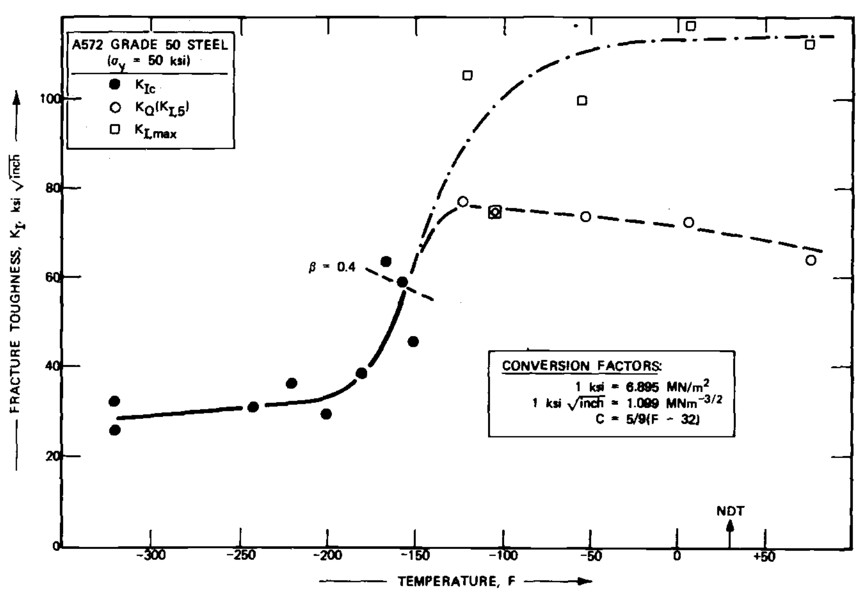

FIG. 22—*Results of static fracture-toughness tests of A572 Grade steel (σ_y = 50 ksi).*

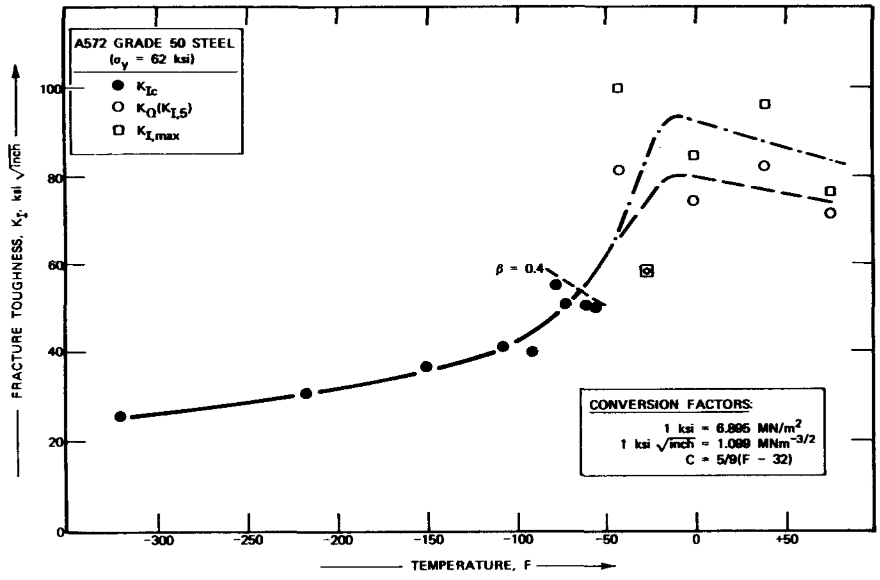

FIG. 23—*Results of static fracture-toughness tests of A572 Grade 50 steel (σ_y = 62 ksi).*

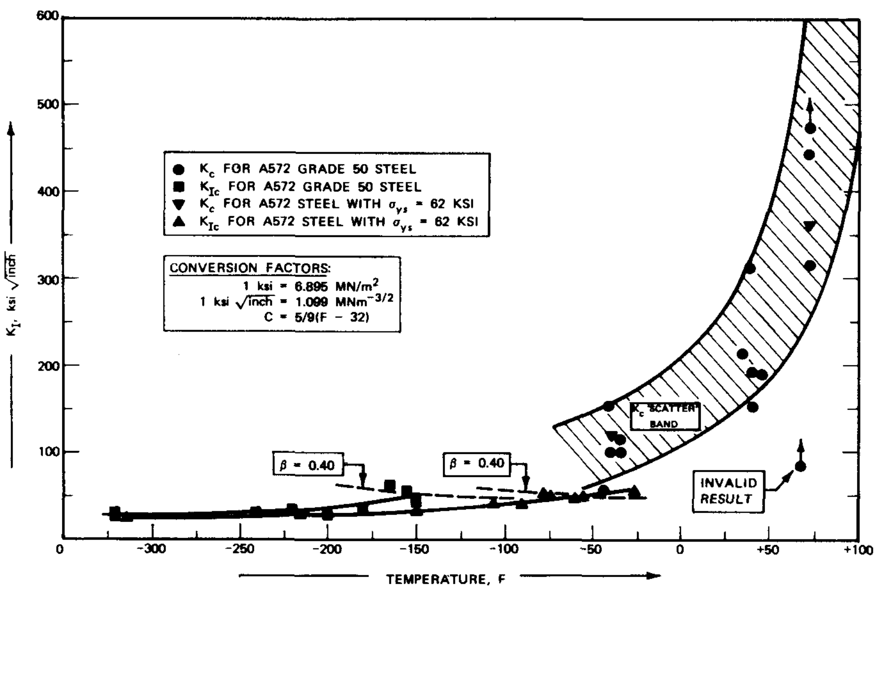

FIG. 24—*Summary comparisons of K_c and K_{Ic} behavior obtained from 1.5-in.-thick plates of A572 steel.*

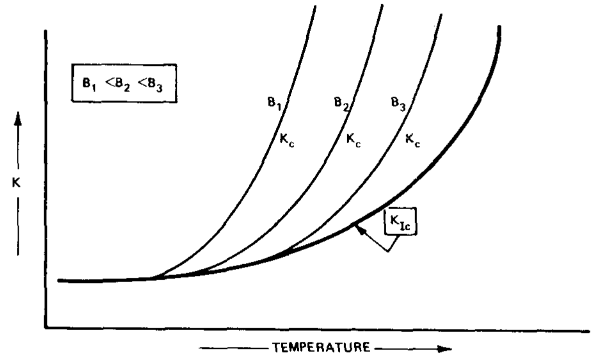

A. SCHEMATIC OF RELATIONSHIPS BETWEEN K_c AND K_{Ic} IN A K_{Ic} TRANSITION TEMPERATURE REGION

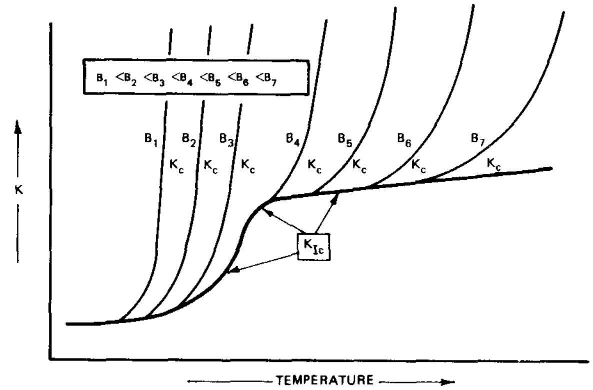

B. SCHEMATIC OF RELATIONSHIPS BETWEEN K_c AND K_{Ic} FOR BOTH A K_{Ic} TRANSITION TEMPERATURE REGION AND A HIGHER K_{Ic} SHELF (GRADUALLY INCREASING) TEMPERATURE REGION

FIG. 25—*Schematics of relationships between K_c and K_{Ic}.*

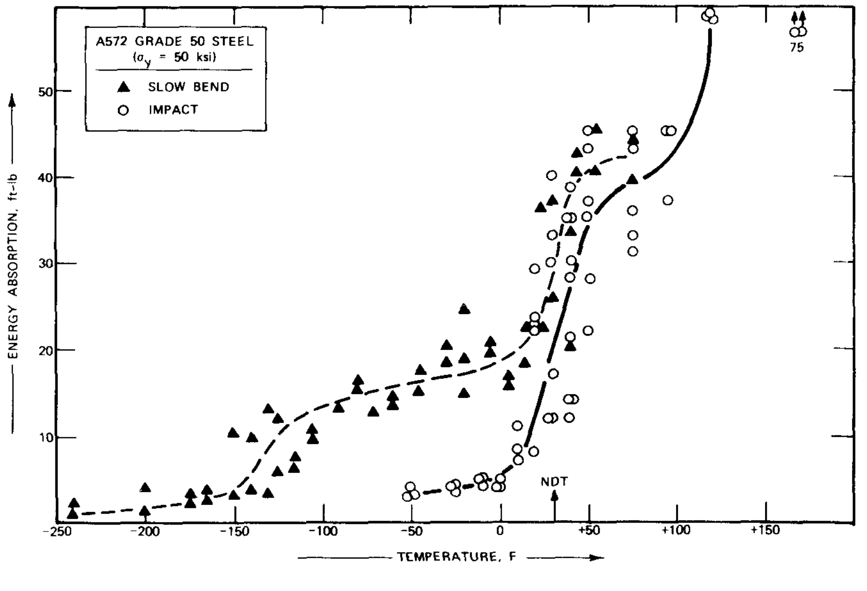

FIG. 26—*Longitudinal Charpy V-notch energy absorption for impact and slow-bend tests of standard CVN specimens.*

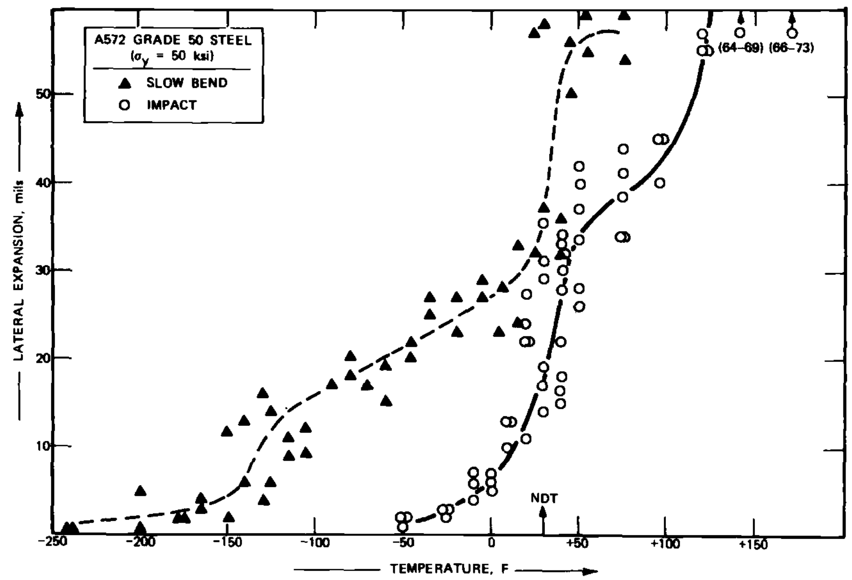

FIG. 27—*Longitudinal Charpy V-notch lateral expansion for impact and slow-bend tests of standard CVN specimens.*

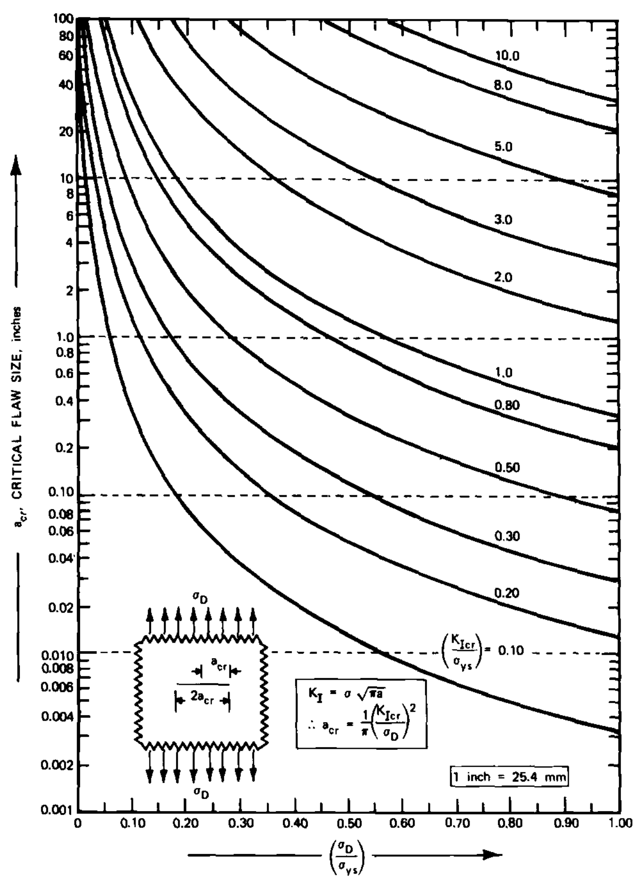

FIG. 28—*Critical flaw size (a_{cr}) requirements for the initiation of a critical event (K_{Icr}) for cracks contained in an infinite center-cracked tension (CCT) specimen and subjected to a uniform tension stress (σ_D) applied remotely.*